NASA TR R-384

A STUDY OF FM THRESHOLD EXTENSION TECHNIQUES

by G. D. Arndt and F. J. Loch

Manned Spacecraft Center
Houston, Texas 77058

1. Report No. NASA TR R-384	2. Government Accession No.	3. R	
4. Title and Subtitle A STUDY OF FM THRESHOLD EXTENSION TECHNIQUES		5. Report Date April 1972	
		6. Performing Organization Code	
7. Author(s) G. D. Arndt and F. J. Loch, MSC		8. Performing Organization Report No. MSC S-306	
		10. Work Unit No. 914-50-50-17-72	
9. Performing Organization Name and Address Manned Spacecraft Center Houston, Texas 77058			
		11. Contract or Grant No.	
12. Sponsoring Agency Name and Address National Aeronautics and Space Administration Washington, D.C. 20546		13. Type of Report and Period Covered Technical Report	
		14. Sponsoring Agency Code	

15. Supplementary Notes

16. Abstract

Investigations into the FM threshold phenomenon have resulted in the development of several signal processing techniques that can be implemented at the output of any FM demodulator, including phase lock loop and FM feedback demodulators, to provide improved system performance. These techniques are based on the distinguishing characteristics of the demodulator output noise below threshold. Performance improvement and threshold extension are achieved by operating on the demodulator output signal and noise such that the threshold noise impulses are eliminated.

The characteristics of three postdetection threshold extension techniques are evaluated with respect to the ability of such techniques to improve the performance of a phase lock loop demodulator. These techniques include impulse-noise elimination, signal correlation for the detection of impulse noise, and delta modulation signal processing.

Experimental results from signal-to-noise ratio data and bit error rate data indicate that a 2- to 3-decibel threshold extension is readily achievable by using the various techniques. This threshold improvement is in addition to the threshold extension that is usually achieved through the use of a phase lock loop demodulator.

17. Key Words (Suggested by Author(s)) ° FM Threshold Extension ° Impulse Noise Elimination ° Correlation Detection ° Delta Modulation Encoding		18. Distribution Statement		
19. Security Classif. (of this report) None	20. Security Classif. (of this page) None		21. No. of Pages 56	22. Price* $3.00

CONTENTS

FIGURES

A STUDY OF FM THRESHOLD EXTENSION TECHNIQUES

By G. D. Arndt and F. J. Loch
Manned Spacecraft Center

SUMMARY

A laboratory investigation of the FM threshold phenomenon has resulted in the development of several signal processing techniques that can be implemented at the output of any FM demodulator (including the phase lock loop and frequency modulation feedback demodulator) to provide improved system performance. These techniques are based on the distinguishing characteristics of the demodulator output noise below threshold. Performance improvement and threshold extension are achieved by operating on the demodulator output signal and noise such that the threshold noise impulses are reduced.

The characteristics of three postdetection threshold extension techniques are evaluated with respect to the capability of each technique to improve the performance of a phase lock loop demodulator. These techniques include impulse noise elimination, signal correlation for detecting impulse noise, and delta modulation signal processing.

The results of qualitative waveform analysis tests, signal-to-noise ratio tests, and bit error rate tests are used to evaluate the relative performance of each threshold extension device. A mathematical model is developed for the delta modulator threshold extension technique to describe the improvement in signal-to-noise ratio performance obtainable with the technique.

INTRODUCTION

Threshold extension can be obtained in most FM systems by implementing a phase lock loop (PLL) or frequency modulation feedback (FMFB) demodulator in place of a standard frequency discriminator. The amount of realizable predetection signal-to-noise ratio (SNR) improvement obtained with a PLL or FMFB demodulator over the standard discriminator usually is 2 or 3 decibels. However, the performance of these threshold extension demodulators also is limited by the FM threshold phenomenon, which occurs when the input SNR falls below a certain value.

A laboratory investigation of the FM threshold phenomenon resulted in the development of several signal processing techniques that can be implemented at the output of any FM demodulator (including the PLL and FMFB) to provide improved system performance. These techniques are based on the distinguishing characteristics of the demodulator output noise below threshold. Performance improvement and threshold

extension are achieved by operating on the demodulator output signal and noise such that the threshold noise impulses are reduced.

The techniques, which include a basic impulse noise elimination system, a signal correlation system for detecting impulse noise, and a delta modulation (DM) threshold extension device, are described and compared in this report. Test results are presented for each technique.

The basis for the theoretical work described in the following sections is taken from the classical impulse noise analysis of S. O. Rice (ref. 1). The results of Rice's analysis are expanded to include the effects of quantization noise and reduction in impulse noise power for the DM threshold extension technique.

SYMBOLS

A	amplitude of the voltage signal into the demodulator, V
A_m	amplitude of the output modulating signal, V
A_{max}	maximum allowable signal amplitude that can be encoded without slope overload, V
a	discriminator constant, V/rad/sec
BW_{IF}	intermediate frequency bandwidth, Hz
BW_{in}	input bandwidth, Hz
BW_{loop}	loop bandwidth of the phase lock loop demodulator, Hz
BW_o	output bandwidth, Hz
BW_{o_2}	second subcarrier output bandwidth, Hz
BW_s	shaping filter bandwidth, Hz
b	number of unit areas $S_A \tau_{\Delta M}$ contained in the first encoding level
$C(t)$	unmodulated carrier into the demodulator
c	number of unit areas in the N_Lth encoding level
erfc	complementary error function

f	frequency, Hz
f_{co}	cut-off frequency, Hz
f_m	modulating frequency, Hz
f_{max}	maximum allowable signal frequency that can be encoded without slope overload, Hz
f_o	center frequency
f_p	clock pulse repetition rate, Hz
f_{sc}	subcarrier frequency, Hz
f_{sc_1}, f_{sc_2}	frequency of subcarrier 1 and 2, Hz
$G_{N_q}(f)$	quantization noise spectral density, dBm/Hz
$G_{N_s}(f)$	impulse noise spectral density, dBm/Hz
$G_{N_{TH}}(f)$	thermal noise spectral density, dBm/Hz
IF	intermediate frequency, Hz
I(t)	uncoded impulse
K	noise impulse reduction factor due to delta modulation encoding
m(t)	modulating signal
$\hat{m}(t)$	encoded estimate of the modulating signal
N_L	number of encoding levels (steps) per impulse
N(t)	input noise voltage to the demodulator, V
n(f)	output noise power spectral density, dBm/Hz
n_s	number of impulses per second
P	relative power of the encoded impulses, dBm

3

P_{N_q} quantization noise power at the output of the delta modulator, dBm

P_{N_s} impulse noise power at the output of the delta modulator, dBm

$P_{N_{TH}}$ thermal noise power at the output of the delta modulator, dBm

P_{S_o} output signal power, dBm

$R(t)$ magnitude of the resultant carrier-plus-noise waveform, V

S_A step amplitude of the delta modulator clock pulses, V

SNR_{in} input signal-to-noise ratio, dB

SNR_o output signal-to-noise ratio, dB

T_s mean time between impulses, sec

t time variable

(t) function of time

$X(t), Y(t)$ independent random variables, V

V_s amplitude of the output impulse, V

Δf frequency deviation, Hz

Δf_1 carrier frequency deviation, Hz

Δf_2 subcarrier frequency deviation, Hz

$\Delta \omega$ radian frequency deviation, rad/sec

$\epsilon(t)$ error voltage, V

Σ signal summer

τ delay time, sec

τ_m modulating signal duration, sec

τ_s impulse duration, sec

4

$\tau_{\Delta M}$ time period of the delta modulator clock pulse, sec

ϕ_{IF} two-sided noise spectral density, dBm/Hz

$\phi(t)$ phase of the resultant $R(t)$ with respect to the carrier, rad

ω_c radian carrier frequency, rad/sec

ω_m modulation frequency, rad/sec

Subscripts:

s   uncoded impulse

Δs   encoded impulse

THE FM THRESHOLD PHENOMENON

Background

By definition, the criteria for evaluating the performance of an FM demodulator are based on the capability of the device to provide a linear relationship between the output and input signal-to-noise ratios. However, the useful operating range of all FM demodulators is limited by the fact that this linear relationship, or transfer characteristic, becomes nonlinear below a certain value of input SNR. This input SNR value is called the point of threshold for the demodulator.

Because it is difficult to determine the exact value of input SNR that divides the linear and nonlinear regions of the performance curve, a reasonable criterion for the determination of the threshold point must be defined. One accepted definition of FM threshold is based on the graphical determination of the specific input SNR value for which the corresponding output SNR occurs exactly 1 decibel below an extension of the linear portion of the transfer curve. This method of defining FM threshold, which is illustrated in figure 1, is used consistently in this document.

The occurrence of threshold in an FM system also can be defined in terms of the demodulator output noise characteristics. In general, when the demodulator is operating with values of input SNR greater than 10 decibels, the output noise spectrum is parabolic, and the amplitude distribution is Gaussian. As the input SNR decreases, the output noise voltage is punctuated with occasional high-amplitude noise spikes that have either positive or negative polarity. These noise impulses become more frequent as the input SNR is reduced to values below 10 decibels. For the region of input SNR between 0 and 10 decibels, the output noise power increases at a rate such that the slope of the SNR transfer curve becomes much more severe than the slope of the linear portion. Thus, a small change in input SNR results in a relatively large change in output SNR, as illustrated in figure 1. The difference in the relative contribution of Gaussian noise and impulse noise is evident from the spectral characteristics of each in figure 2.

5
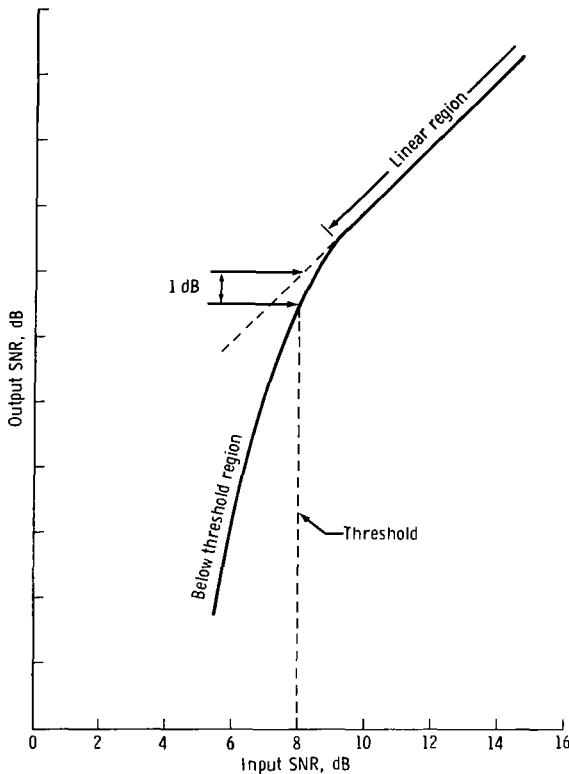
Figure 1. - Graphical determination of the FM threshold for a typical demodulator SNR transfer drive.
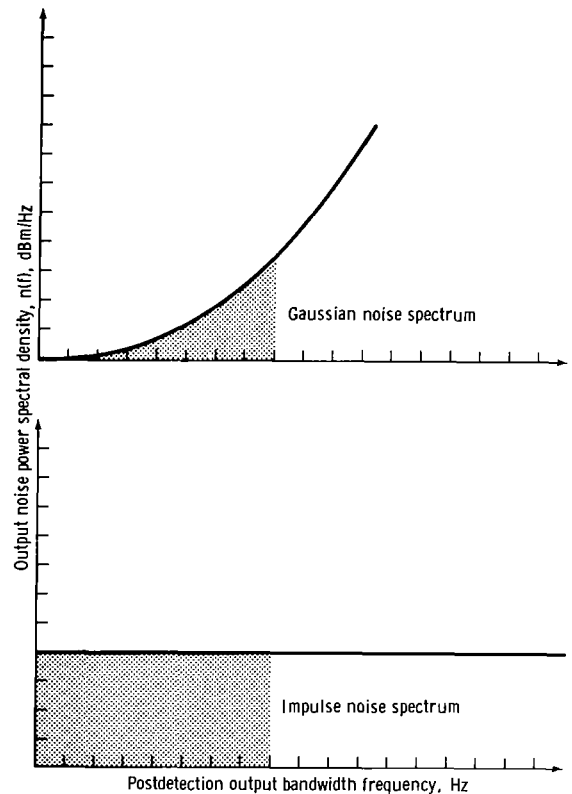
Figure 2. - Output noise characteristics of the FM demodulator.

The energy contained in the individual noise spikes (called impulse or click noise) at the output of an FM demodulator contributes significantly to the total output noise power. In addition, the impulsive nature of click noise causes it to be much more degrading to the demodulated signal than is the Gaussian output noise. Although impulse noise is not the only phenomenon that causes FM threshold, it is a primary factor contributing to the occurrence of threshold in an FM system.

Characteristics of Impulse Noise

The detection and subsequent elimination of impulse noise can be simplified by first determining the distinguishing characteristics of these impulses. Consider an unmodulated signal at the input of an ideal FM discriminator where the carrier is represented as C(t), the amplitude as A, and the radian carrier frequency as $\omega_c t$.

$$C(t) = A \cos \omega_c t \qquad (1)$$

6

The input noise to the discriminator can be represented in quadrature form by

$$N(t) = X(t)\cos \omega_c t + Y(t)\sin \omega_c t \tag{2}$$

where $N(t)$ is the input noise and $X(t)$ and $Y(t)$ are independent random variables. Therefore, the total input carrier plus noise is

$$C(t) + N(t) = [A + X(t)]\cos \omega_c t + Y(t)\sin \omega_c t \tag{3}$$

which also can be expressed

$$C(t) + N(t) = R(t)\cos\left[\omega_c t + \phi(t)\right] \tag{4}$$

where $R(t)$ is the magnitude of the resultant carrier-plus-noise waveform and $\phi(t)$ is the phase of the resultant $R(t)$ with respect to the carrier. The FM demodulator detects the frequency of the signal by differentiating the phase of the received signal plus noise. The phase of the signal-plus-noise waveform can be obtained from equation (3).

$$\phi(t) = \tan^{-1} \frac{Y(t)}{A + X(t)} \tag{5}$$

For high signal-to-noise ratios, the assumption that $A \gg X(t)$ can be made. Therefore,

$$\phi(t) = \tan^{-1}\frac{Y(t)}{A} \doteq \frac{Y(t)}{A} \tag{6}$$

The phasor relationship that exists between A, $X(t)$, $Y(t)$, $R(t)$, $N(t)$, and $\phi(t)$ is as shown in figure 3. The fluctuation of the Gaussian distributed random variables $X(t)$ and $Y(t)$ causes the angle $\phi(t)$ to change accordingly.
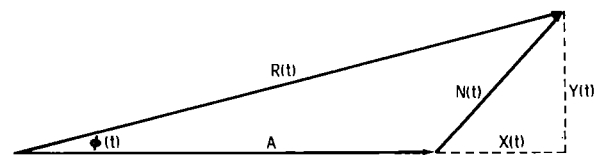
Figure 3. - Phasor representation of A, $X(t)$, $Y(t)$, $R(t)$, $N(t)$, and $\phi(t)$.

The impulse event takes place at the FM discriminator input as an interaction between the randomly varying noise envelope and the carrier amplitude that results in a sudden 2π-radian phase excursion of the carrier-plus-noise vectoral resultant $R(t)$ (ref. 1). Both plus and minus 2π-radian

phase excursions can occur with equal probability, which results in a corresponding positive or negative noise spike in the demodulator output.

By using the phasor representation of figure 4, the impulse event can be defined in terms of a $\pm 2\pi$-radian phase excursion by the angle $\phi(t)$. The probability of such a phase excursion increases as the input SNR to the discriminator decreases below 10 decibels. In figure 4, for low values of input SNR, a small change in the phase angle between the noise and carrier waveforms can result in a relatively large change $\Delta\phi(t)$ in the resultant phase angle.

Because the output of an ideal discriminator is proportional to $d\phi(t)/dt$, the 2π-radian phase excursion causes a noise spike of area 2π to occur at the output, as shown in figure 5. It also is possible for the phase angle to experience a phase excursion of 4π, 6π, or even 8π radians. For phase steps exceeding 2π radians, the resulting output noise spike will have a proportionally greater duration before postdetection filtering. Figures 6 to 9 show the impulse waveform before and after postdetection filtering. Several photographs are provided to illustrate the higher order impulses since each unfiltered waveform is unique. Impulses resulting from a $\pm 2\pi$-radian phase excursion are represented in figure 6. These noise spikes are designated as first-order impulses because the spikes are the result of the minimum impulse-producing phase excursions. Some higher order impulses also are present in figures 6 to 9; the impulses indicated in the figure legends are shown in the left portion of the photographs. Second-order impulses (4π radians) are represented in figure 7. The duration of the second-order impulses is approximately twice that of the first-order impulses at the unfiltered output of the demodulator. The noise contribution of the second-order impulses is correspondingly greater than that of the first-order impulses.

The difference between first- and second-order impulses can be distinguished easily at the output of the demodulator postdetection filter by observing the relative amplitude of the spikes. The cut-off frequency of the low-pass filter determines the duration of the output noise spikes so that both first- and second-order impulses have the same duration at the filter output.
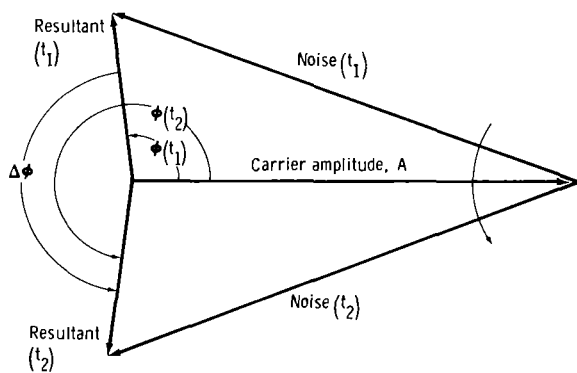
Figure 4. - Phasor representation of noise, carrier, and resultant below FM threshold.
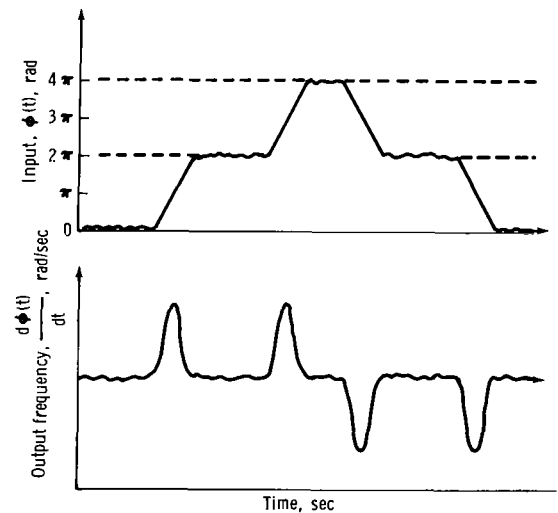
Figure 5. - Relationship between $\pm 2\pi$-radian phase excursions and resulting impulses of area 2π.
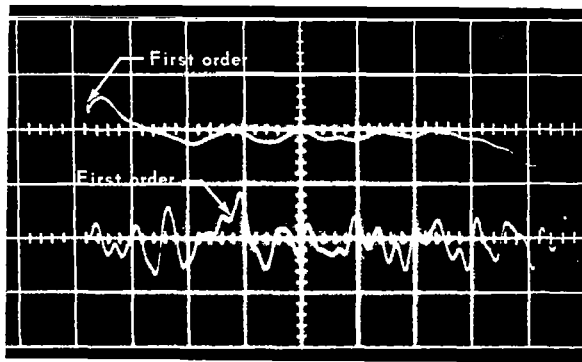
Grid interval = 1 μsec

Figure 6. - First-order impulse wave-
form. The upper trace is filtered; the
lower trace is unfiltered.
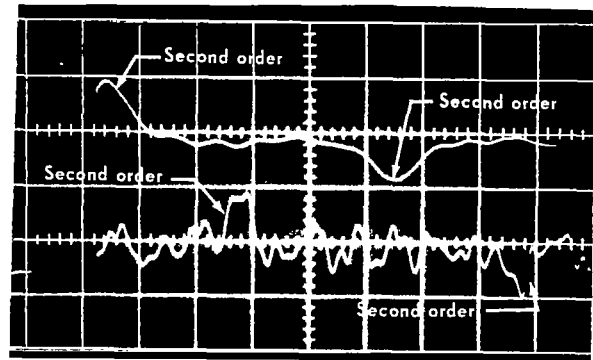
Grid interval = 1 μsec

Figure 7. - Second-order impulse wave-
form. The upper trace is filtered; the
lower trace is unfiltered.
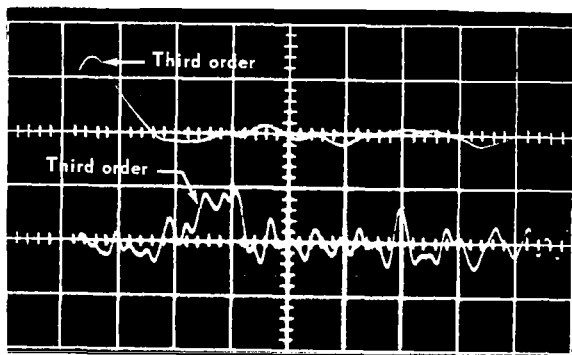
Grid interval = 1 μsec

Figure 8. - Third-order impulse wave-
form. The upper trace is filtered; the
lower trace is unfiltered.
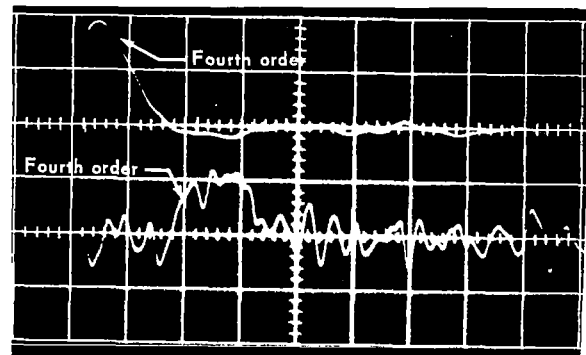
Grid interval = 1 μsec

Figure 9. - Fourth-order impulse wave-
form. The upper trace is filtered; the
lower trace is unfiltered.

Therefore, the difference in duration between the first- and second-order impulses at
the unfiltered output is translated to an amplitude difference in the filtered output. The
relative amplitude and duration relationships between the different orders of filtered
and unfiltered impulse waveforms are summarized as follows.

9

Impulse order	Unfiltered duration, 10^{-6} sec	Filtered relative amplitude, cm
First	0.5	0.5
Second	1.0	1.0
Third	1.5	1.5
Fourth	2.0	2.0

Third- and fourth-order impulse waveforms at the demodulator output are shown in figures 8 and 9. These higher order impulses occur only for very low values of input SNR, and, for practical considerations, the contribution of these impulses to the total output noise power can be neglected. In most cases, the degradation of the demodulator output below threshold will be caused primarily by the occurrence of first-order impulses.

THRESHOLD EXTENSION TECHNIQUES

Basic Impulse Noise Eliminator

In the discussion of FM threshold in the preceding section, the presence of high-amplitude impulse noise in the demodulator output was recognized as a primary factor contributing to the occurrence of threshold in an FM system. Certain distinguishing characteristics of impulse noise provide a basis for practical techniques that can be implemented at the output of an FM demodulator to extend the threshold performance of the system. The threshold extension technique described in this section is based on the accomplishment of two steps.

1. Detection of the noise impulses in the demodulator output by distinguishing the impulses from the demodulated signal and from the low-level Gaussian noise

2. Utilization of the detected impulse noise information to perform an impulse elimination operation on a delayed version of the demodulator output

Impulse detection. - Detection of the noise impulses is simplified if, as is true in most cases, the peak amplitude of the impulse noise is greater than that of the modulating signal and the Gaussian noise in the demodulator output. A typical example that illustrates this point is presented in figure 10.

The upper waveform in the photograph represents the signal-plus-noise output bandwidth BW_o of a 500-kilohertz low-pass postdetection filter; the lower sweep represents the signal plus noise that is present in the unfiltered (4 megahertz) demodulator output. The sweeps in each photograph are alined such that the relationship between
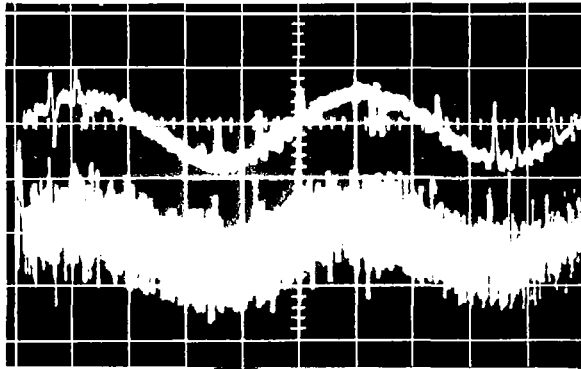
Grid interval = 20 μsec

Figure 10. - Demodulated signal-plus-noise waveform with and without post-detection filtering. The upper trace is filtered (BW_O = 500 kHz); the lower trace is unfiltered (BW_O = 4 MHz).

Conditions: f_m = 10 kHz, Δf = 1 MHz.

unfiltered and filtered waveforms can be observed for a particular impulse event. Note that the postdetection filter acts to attenuate and to broaden the impulse waveform.

A certain number of high-amplitude noise spikes, which are present on the unfiltered waveform, have the same amplitude as the noise impulses but do not result in a corresponding impulse on the filtered output waveform. These noise spikes belong to the Gaussian portion of the unfiltered output noise. The energy of the spikes is concentrated primarily in frequencies above the cut-off of the low-pass postdetection filter because of the parabolic spectrum of the Gaussian noise.

The probability of detecting these non-impulse-producing noise spikes can be minimized by implementing a postdetection filter to attenuate the higher frequency Gaussian noise components. (A 2-megahertz low-pass filter has been found experimentally to preserve the relative high-amplitude characteristic of the impulse-producing noise.)

Impulse elimination. - The following steps summarize the operation of a basic impulse noise elimination threshold extension device, as shown in figure 11.

1. The output of an FM demodulator is passed through a low-pass filter, which has a cut-off frequency f_{co} much greater than the maximum modulation signal frequency f_m. This impulse-shaping filter determines both the amplitude and duration of the threshold noise impulse. The primary purpose of this filter is to maximize the ratio of the amplitude of the impulse noise to that of the Gaussian noise.

2. The filtered demodulator output is split into two channels.

3. Channel A is fed to a pair of level detectors (Schmitt triggers) that are adjusted to trigger only on impulse noise. One level detector is used for positive impulses; the other detects negative impulses. The reference (trigger) voltage levels are established such that only impulse-producing noise spikes will be detected. The output of each level detector triggers a pulse generator that produces a single pulse for each detected noise impulse.

4. Channel B is delayed by the time τ, which is approximately equal to $1/f_{co}$ (the duration of a noise impulse). Then, the delayed channel B is supplied to a follow-and-hold circuit, which is gated by the output of the channel A pulse generators. The follow-and-hold circuit consists of an amplifier with an output that can be gated off for

11

Figure 11.- Basic impulse noise elimination threshold extension system.

a predetermined time and a "holding" circuit that provides a constant output voltage during the time the amplifier is biased off. The output voltage of the holding circuit corresponds to the demodulator output just before the beginning of the impulse. The channel B delay is selected such that the gating pulse from the impulse noise detection channel initiates a hold just prior to the arrival of the actual impulse into the follow-and-hold circuit. The effect of this system is to provide an approximation of the modulation as a substitute for the high-amplitude noise impulse in the demodulator output.

One specific hold duration can be used to eliminate each noise impulse because the time duration of all threshold impulses is determined by the shaping filter. Because the cut-off frequency of the impulse shaping filter is much greater than the maximum modulation frequency, the impulse duration and hold time are small compared with the modulation frequency. A postdetection low-pass filter is used at the output of the impulse noise eliminator to provide smoothing and additional noise filtering.

A simple amplitude detection technique is used in the threshold extension system shown in figure 11 to determine the occurrence of threshold impulse noise in the output of the FM demodulator. A low-pass filter shapes the amplitude of the impulses and thereby increases the probability of correct detection. This detection scheme performs effectively with FM systems that have relatively small frequency deviations, because the peak amplitude of the demodulated signal generally is below the impulse noise amplitude at the output of the low-pass impulse-shaping filter.

An operational threshold extension device based on the system represented in figure 11 has been fabricated and tested at the NASA Manned Spacecraft Center (MSC). The results of laboratory tests in which the device has been used at the output of a PLL demodulator are indicative that such a system is practical for obtaining additional threshold extension beyond that usually provided by the demodulator. These results are discussed in the section entitled "Experimental Results."

12

Signal Correlation for Detection of Impulse Noise

The effectiveness of the basic impulse detection scheme previously discussed is constrained by the preciseness to which the amplitude levels must be set and the long-term stability requirements for the frequency deviations of the modulating signals. The possibility exists that the level detectors will trigger on a modulation peak and provide a false gating pulse to the follow-and-hold circuit.

A signal correlation technique that significantly increases the probability of correct impulse noise detection is presented in figure 12. The signal plus noise at the output of an FM demodulator is compared with itself (inverted) and delayed by time τ. If no impulse is present, the correlation voltage is approximately zero. If an impulse is present, the correlation voltage will appear as a positive and a negative impulse (doublet) around a zero mean, representing the modulating signal. Then, it becomes a simple matter to detect and eliminate the impulses by using conventional amplitude-sensitive level detectors.
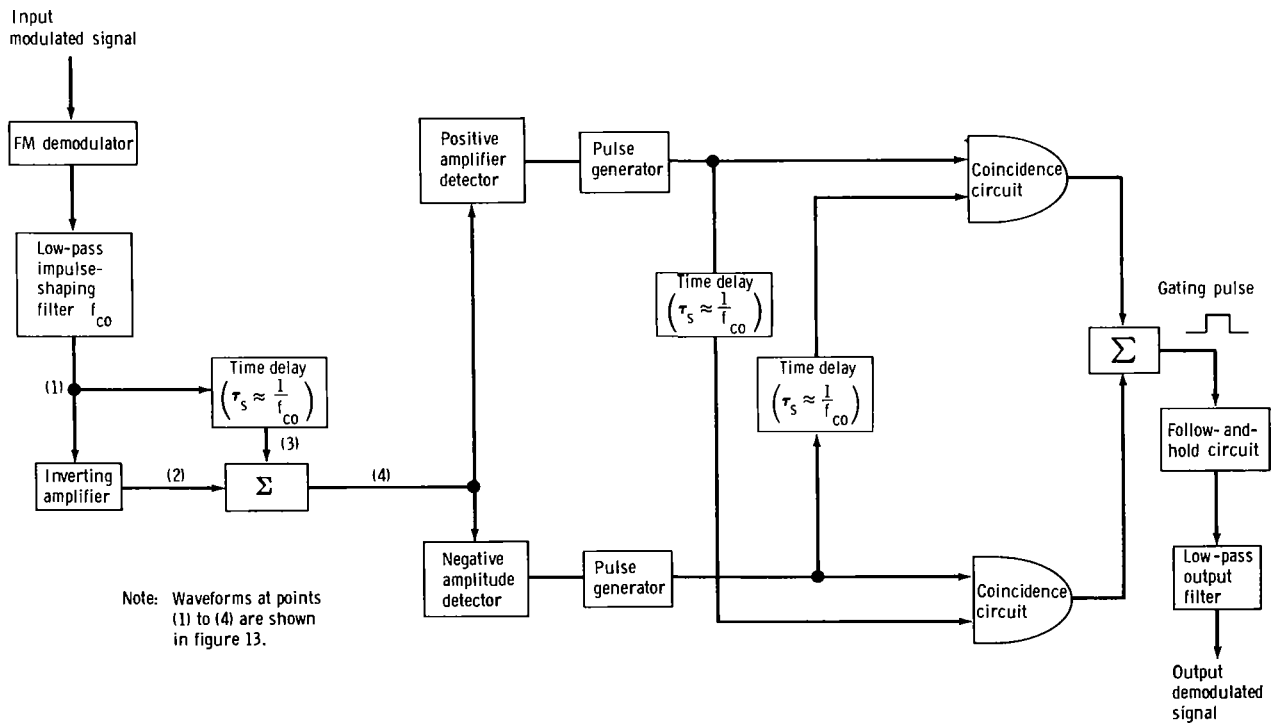
Figure 12. – System for correlation detection and impulse noise elimination.

For this system, a low-pass filter is used at the output of an FM demodulator to shape the noise impulse and set the pulse duration τ_s. The pulse duration is small in comparison with the period of the modulating signal; that is, $\tau_s \ll \tau_m$. Then, the

output of the impulse-shaping filter is split into two channels. Channel A is inverted and channel B is delayed by time τ_s, which is approximately equal to the duration of a noise impulse. The two channels are summed, resulting in a low-amplitude residual modulation waveform that contains high-amplitude bipolar doublets. Figure 13 shows the representative signal-plus-noise waveform at various points in the correlation detection system. Each bipolar doublet represents a single noise impulse.

The doublets are detected by a pair of positive and negative level detectors that are adjusted to trigger only on the high-amplitude components. The output of the level detectors is fed into a pair of pulse generators, which provide two pulses for each detected doublet. Next, a coincidence gate is used to determine the occurrence of a noise impulse and to generate a signal gating pulse for each detected doublet. The coincidence gate logic diagram is shown in figure 14. After the impulse is detected, it must be eliminated from the output signal.

(1) Output of low-pass impulse-shaping filter

(2) Output of inverting amplifier

(3) Output of delay line

(4) Output of summer
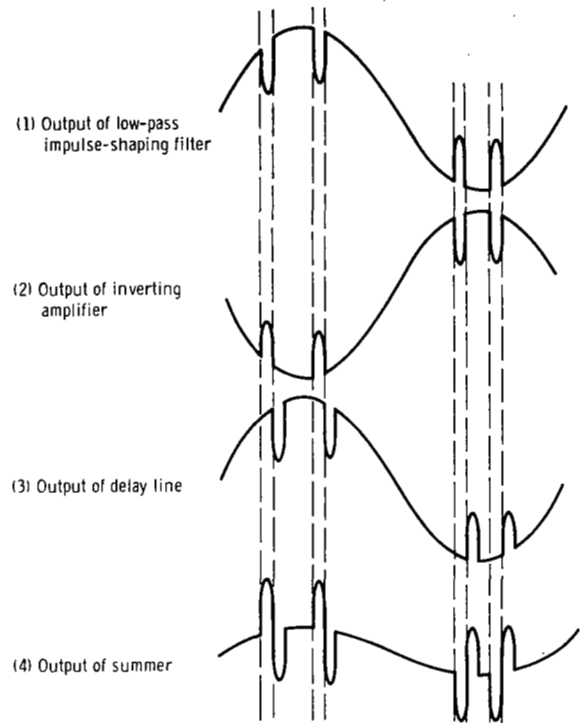
Figure 13. - Waveform representation for correlation detection system.
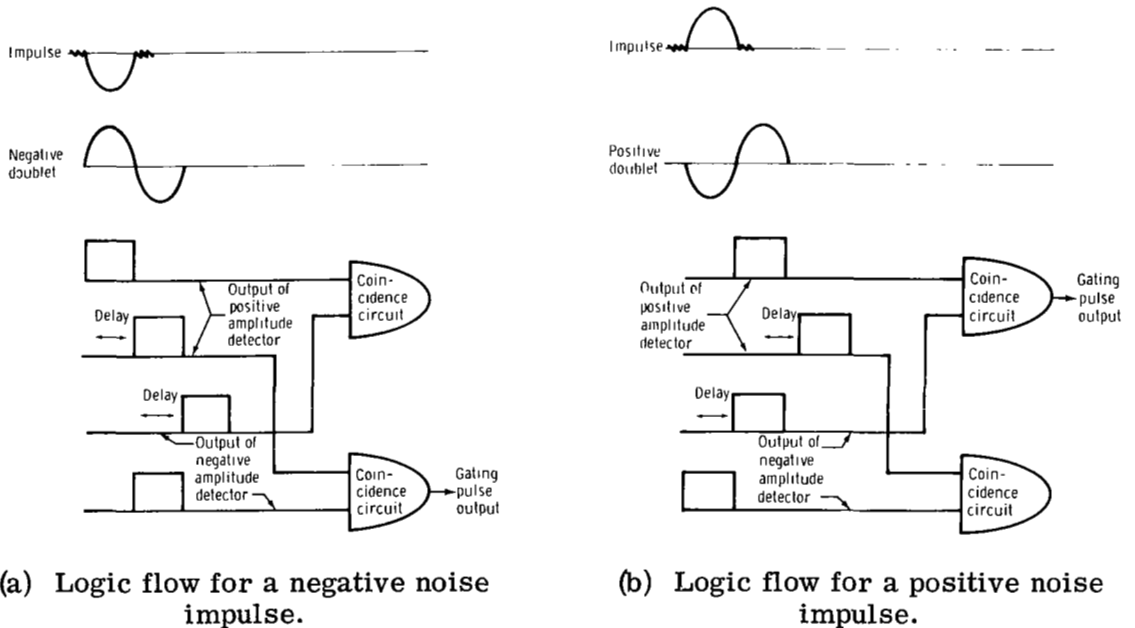
(a) Logic flow for a negative noise impulse.

(b) Logic flow for a positive noise impulse.

Figure 14. - Coincidence gate logic for a correlation detection system.

14

An external impulse elimination device, which has an appropriate signal delay to allow time for the correlation detector to process the impulse, is used. The output pulse from the coincidence detector is used to gate a follow-and-hold circuit. The hold condition exists for approximately the duration of the impulse. The effect of the system is to provide an approximation of the modulation as a substitute for the high-amplitude noise impulse in the output signal. A postdetection filter is used to provide additional noise filtering and smoothing.

Delta Modulation Threshold Extension Technique

Detected impulse noise information is used in the threshold extension techniques discussed in the previous paragraphs to activate a follow-and-hold noise elimination circuit. These techniques are limited primarily by the efficiency of the impulse noise detection schemes. An alternate approach to threshold extension has been developed in which the characteristics of a basic DM system in a signal processing technique are used at the output of an FM demodulator.

The main advantage of the DM threshold extension technique is that the need for impulse noise detection as an integral part of the operation is eliminated. With the DM technique, threshold extension is accomplished by processing the demodulated signal-plus-noise output of a demodulator such that the noise impulses are ignored rather than detected. The application of the basic DM technique to obtain threshold extension is discussed in the following section.

Basic DM system. - Delta modulation is an encoding technique that can be used to convert an analog signal into a binary bit stream. A block diagram for a basic DM system is shown in figure 15. The analog signal input to the delta modulator is represented
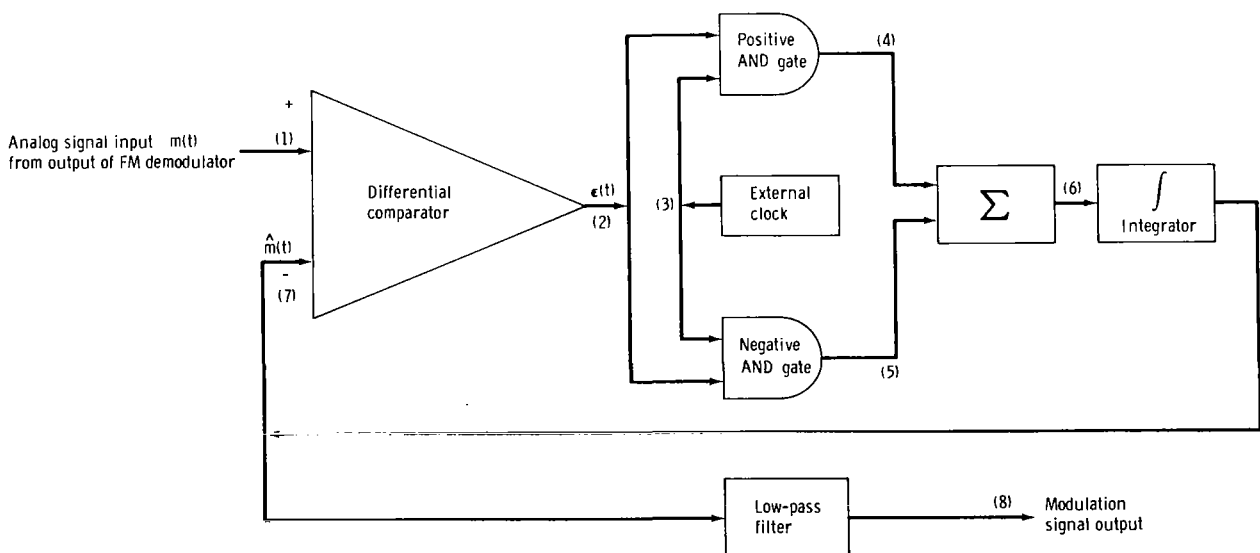
Figure 15. - Basic DM threshold extension system. Signal flow at points (1) to (8) is shown in figure 16.

as m(t) and the estimate of m(t) is designated $\hat{m}(t)$. The signals m(t) and $\hat{m}(t)$ are fed into a differential comparator, which provides a positive voltage output when $[m(t) - \hat{m}(t)] > 0$ and a negative voltage output when $[m(t) - \hat{m}(t)] < 0$. The bilevel output of the differential comparator and clock pulses from an external generator are routed to a pair of AND gates. The AND gates are biased such that one gate provides a positive output pulse whenever a clock pulse and a positive voltage level are present simultaneously at the input to the gate. The second AND circuit is biased to provide a negative output pulse whenever a clock pulse and a negative voltage level are present simultaneously at the gate input. The AND gate output pulses have a duration equal to the clock pulse duration and have a constant positive or negative amplitude. These output pulses are summed to create a continuous binary bit stream, which is provided to an integrator. The output of the integrator represents the encoded analog signal $\hat{m}(t)$. The signal output of the system is obtained by implementing a low-pass filter at the output of the integrator. The filter provides a second integration process that smooths the encoded signal to more closely resemble the input analog signal m(t). A signal-flow diagram for the DM system is shown in figure 16.

The DM system has a characteristic known as slope overload, which results from the use of fixed step duration and amplitude. The slope overload characteristic limits the amplitude and frequency of the encoded signal to specific maximum values, which must be considered in the design of a DM system. The nature of the slope overload for frequency limiting and amplitude limiting is illustrated in figure 17. For a sinusoidal input signal $m(t) = A \sin \omega_m t$, the maximum slope occurs when the waveform passes through the point of zero phase and is equal to $(2\pi f_m)A$.

The slope of the encoded signal $\hat{m}(t)$ is determined by the ratio of the change in amplitude over a given interval. For a fixed step amplitude S_A and a clock pulse repetition rate of f_p, the average slope of m(t) is $S_A f_p$. Therefore, the slope overload condition occurs when the slope of the analog input m(t) exceeds the slope of the encoded estimate $\hat{m}(t)$; that is,

$$2\pi f_m A > S_A f_p \qquad (7)$$

(1) Analog modulation signal input

(2) Output of differential comparator (error between waveforms (1) and (7))

(3) Output of external generator

(4) Output of positive AND gate

(5) Output of negative AND gate

(6) Summer output

(7) Integrator output

(8) Modulation signal output
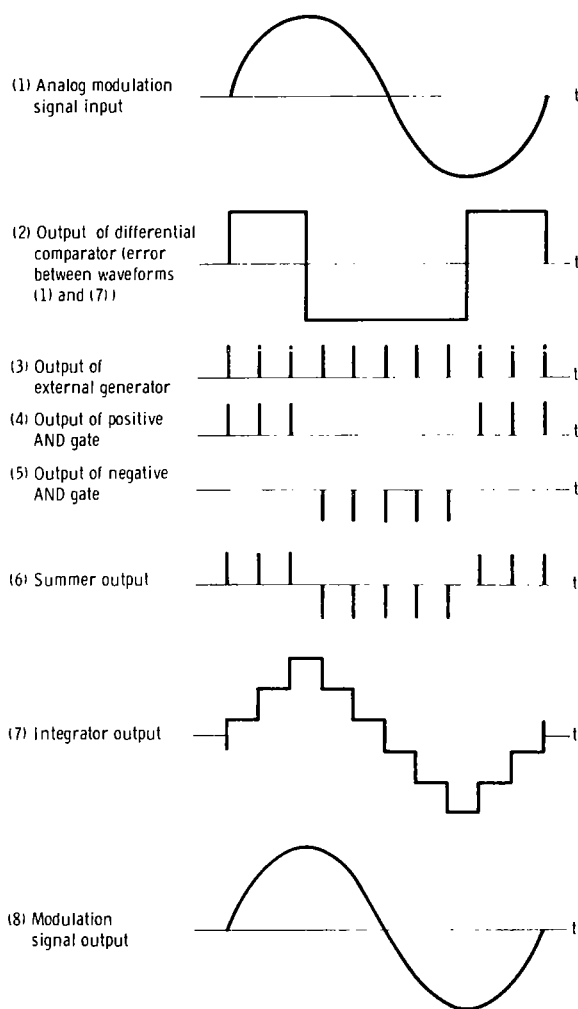
Figure 16. - Signal flow for the DM system.

(a) Normal encoding without slope overload.

(b) Slope overload due to excessive modulation frequency.

(c) Slope overload due to excessive modulation amplitude.

Figure 17. - Slope overload characteristic of the DM system.

From equation (7), the following relationships are obtained.

$$f_{max} = \frac{S_A f_p}{2\pi A} \tag{8}$$

where f_{max} represents the maximum allowable frequency of $m(t)$ that can be encoded without slope overload for fixed values of S_A, f_p, and A; and

$$A_{max} = \frac{S_A f_p}{2\pi f_m} \tag{9}$$

where A_{max} represents the maximum allowable amplitude of $m(t)$ that can be encoded without slope overload.

Threshold extension applications of the DM system. - The basic DM system can be implemented at the output of an analog FM demodulator to provide threshold extension. The DM technique attains threshold extension by encoding the output signal plus noise from the demodulator to suppress noise impulses. To obtain this threshold improvement, the following conditions must be satisfied.

1. The threshold noise impulses have a time duration that is much less than the peak modulation frequency; that is,

$$\tau_s \ll \frac{1}{f_{max}} \tag{10}$$

where τ_s is the noise impulse duration and f_{max} is the maximum modulation frequency at the output of the demodulator.

2. The delta modulator parameters S_A and f_p are selected such that the modulator will experience slope overload for all inputs that have periods much less than f_{max}.

The delta modulator will respond to the modulating signal but is unable to follow the noise impulses. Most of the power in the noise impulses is rejected by the DM system because the system cannot respond to the impulses. Examples of this effect are illustrated in figures 18 and 19. The horizontal sweep has been expanded in figure 19 to allow the resolution of the individual steps of the delta modulator. The upper traces in each figure represent the input to a delta modulator from the filtered output of an FM demodulator operating below threshold. The lower traces represent the delta modulator encoded estimates of the analog input. The parameters were chosen such that the delta modulator is operating at the point of slope overload. The test system configuration for the data shown in figures 18 and 19 is given in figure 20.
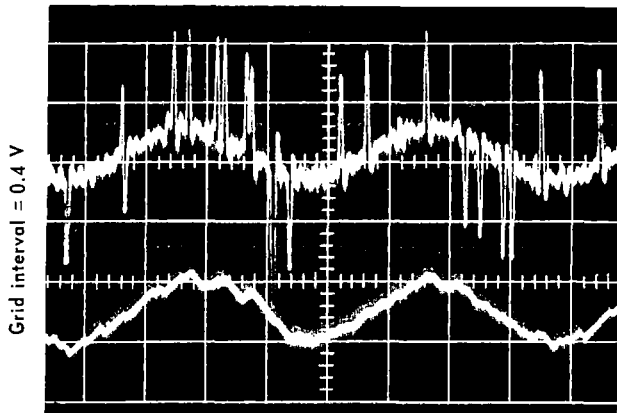
Grid interval = 50 μsec

Figure 18. - Delta modulator noise elimination waveform analysis. The upper trace is the analog input signal plus noise; the lower trace is the encoded output of the delta modulator. Conditions: f_m = 5 kHz, f_p = 500 kHz, S_A = 0.038 V.
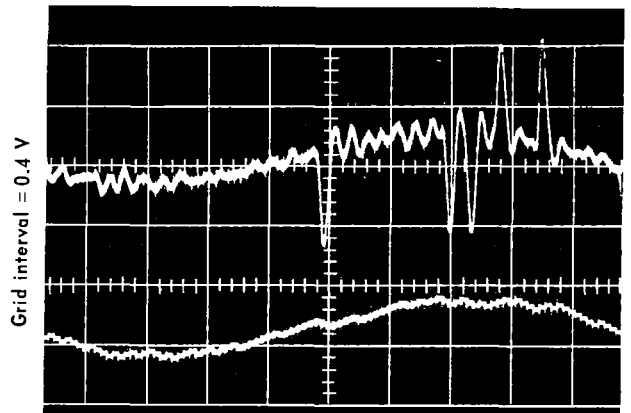
Grid interval ▢ 20 μsec

Figure 19. - Delta modulator noise elimination waveform analysis (horizontal sweep expanded). The upper trace is the analog input signal plus noise; the lower trace is the encoded output of the delta modulator. Conditions: f_m = 5 kHz, f_p = 500 kHz, S_A = 0.038 V.

The modulation frequency is 5 kilohertz, and the low-pass filter preceding the delta modulator has a cut-off frequency of 200 kilohertz. Therefore, each impulse has a duration τ_s of approximately 5 microseconds, and the f_{max} has a period of approximately 0.2 microsecond. These values of τ_s and f_{max} satisfy the condition that $\tau_s \ll 1/f_{max}$.

The effectiveness of DM encoding as a noise-elimination technique is evident in the lower traces of figures 18 and 19. Virtually all of the impulses present on the upper trace input waveforms have been eliminated in the encoding process. However, the effective bandpass of the delta modulator is approximately 5 kilohertz, whereas the bandpass of the input signal plus noise represented by the upper traces is 200 kilohertz. Consequently, a comparison of the two waveforms in figures 18 and 19 can be used only

18
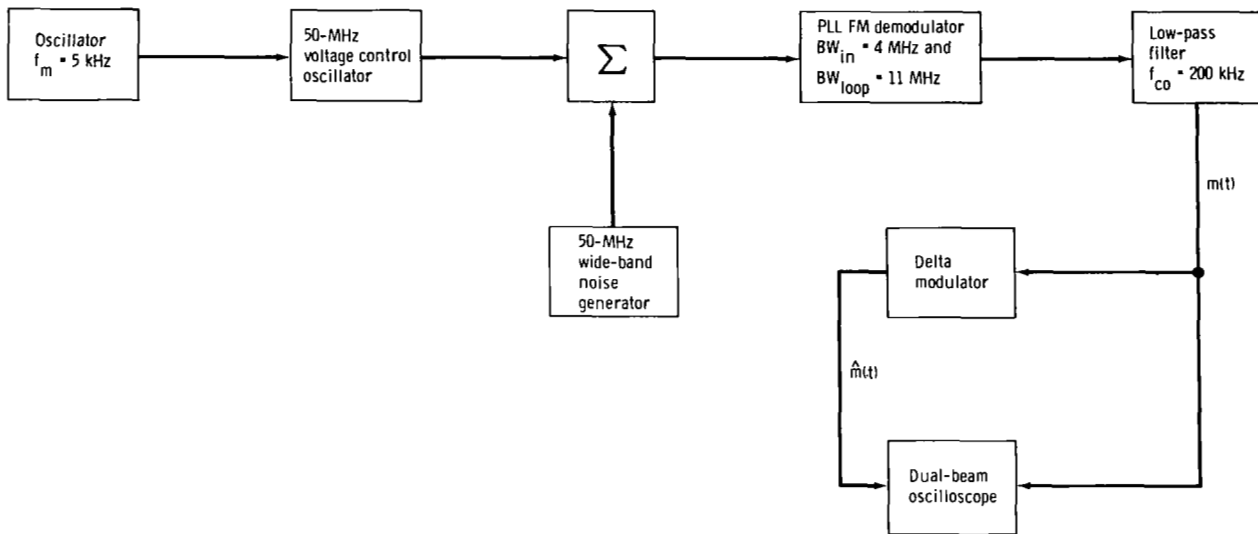
Figure 20. - Delta modulator threshold extension system test configuration.

as a demonstration of the delta modulator impulse noise suppression characteristics rather than as an indication of performance improvement.

The reaction of the delta modulator to individual noise impulses is shown in figure 21. Because the impulse noise duration is approximately 5 microseconds and each delta modulator step has a length equal to $1/f_p$ (2 microseconds), the maximum digression from the signal waveform resulting from the occurrence of a noise impulse period is slightly greater than three times the step amplitude, or 0.075 volt. However, additional noise is added by the delta modulator as it tries to catch up with the signal after
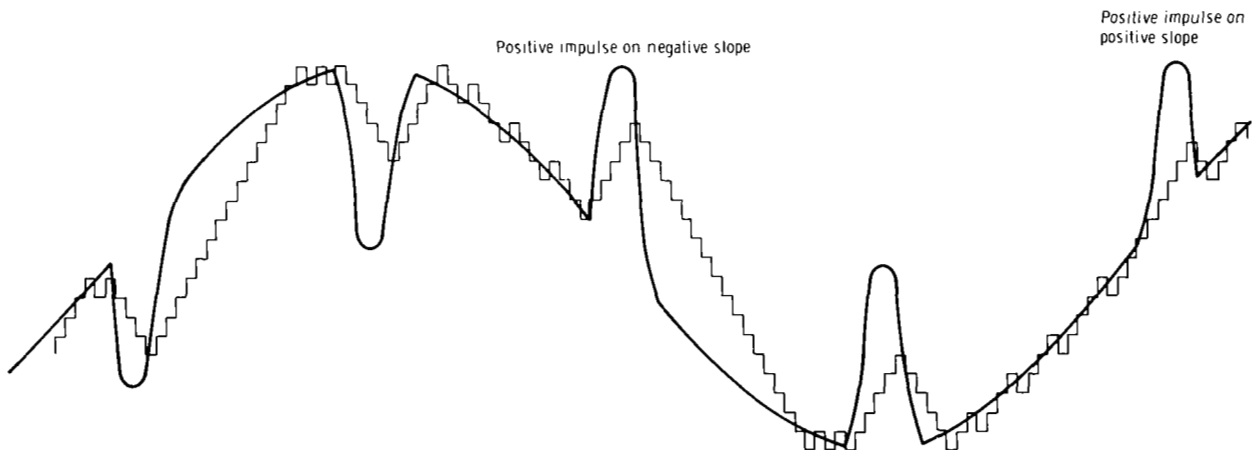
Figure 21. - Effect of signal slope on encoded waveform area.

the impulse has occurred. The quantity of additional noise added by the DM process is dependent on the slope of the signal waveform before and after the noise impulse, as shown in figure 21.

The maximum noise suppression is obtained when the noise impulse polarity has the same sign as the slope of the signal waveform. The converse also is true. The least noise suppression occurs when the noise impulse polarity has the sign opposite to that of the signal waveform slope. For regions in which the signal waveform slope is zero, both positive and negative impulses require the same delta modulator catchup time; therefore, the resulting noise improvement is identical for either case.

It has been found experimentally that most threshold noise impulses occur near the maximum amplitude region (zero slope for a sinusoidal signal) of the signal waveform. This occurrence is to be expected because, in the region of FM threshold, the impulse noise power increases as the frequency of the input is offset from the center frequency of the carrier bandpass filter.

Theoretical Analysis of DM Threshold Extension

The signal-to-noise improvement and subsequent threshold extension of the DM system may be predicted by modifying the classical FM equations derived by Rice (ref. 1). Consider the FM detection system shown in figure 22.
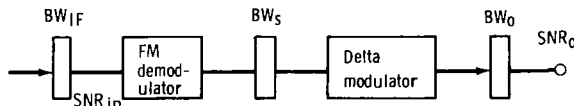
Figure 22. - Diagram of the DM encoding system.

The shaping filter bandwidth BW_s at the output of the demodulator shapes the output noise impulses and determines the impulse period τ_s. Then, the signal plus noise is encoded by the delta modulator. The resultant signal-to-noise performance is measured in the low-pass output filter bandwidth BW_o for which the cut-off is the highest modulation frequency. To determine the transfer function, SNR output compared to SNR input, let the modulating signal be a sinusoid of the modulating amplitude A_m and frequency f_m. The output signal power is

$$P_{S_o} = \overline{m^2(t)} = \frac{A_m^2}{2} = \frac{(a \, \Delta\omega)^2}{2} \tag{11}$$

where $m(t)$ = output signal waveform

a = discriminator constant in V/rad/sec

$\Delta\omega$ = peak frequency deviation $2\pi\,\Delta f$ of the input modulating signal in rad/sec

A_m = amplitude of output modulating signal in volts

The output noise power consists of thermal $P_{N_{TH}}$, impulse P_{N_s}, and quantization P_{N_q} noise contributions; that is, $P_{N_{TH}} + P_{N_s} + P_{N_q}$. Considering the individual noise contributions, the output thermal noise power can be written

$$P_{N_{TH}} = \int_{-BW_o}^{BW_o} G_{N_{TH}}(f)df = \frac{a^2\phi_{IF}}{A^2} \int_{-BW_o}^{BW_o} (2\pi)^2 f^2 df = \frac{8\pi^2}{3}\left(\frac{a^2\phi_{IF}}{A^2}\right) BW_o^3 \qquad (12)$$

where $G_{N_{TH}}(f)$ = thermal noise spectral density

ϕ_{IF} = two-sided noise spectral density

A = amplitude of the voltage signal into the demodulator

BW_o = output modulation bandwidth

Equation (12) is cited in many communication textbooks as the standard expression for FM thermal noise.

The impulse noise can be determined by integrating the power spectral density for an impulse $G_{N_s}(f)$ over the baseband bandwidth. For the experimental tests, the output filter bandwidth BW_o is narrow in comparison with the intermediate frequency bandwidth BW_{IF} (where $BW_o \ll BW_{IF}$). Hence, the spectral components of the impulse noise are approximately constant and equal to $V(j\omega = 0)$, the value of the Fourier transform at $\omega = 0$, over the frequency range of the baseband filter. This can be expressed

$$V(j\omega) \approx V(j\omega = 0) = \int_{-\infty}^{\infty} V(t)e^{j(0)}dt = 2\pi a \qquad (13)$$

where a = discriminator constant in V/rad/sec

2π = area of the input impulse

The total impulse power is written (ref. 2)

$$P_{N_s} = \int_{-BW_o}^{BW_o} G_{N_s}(f)df = \int_{-BW_o}^{BW_o} \frac{(2\pi a)^2}{T_s} df = \frac{(2\pi a)^2}{T_s} 2BW_o$$

$$= (2\pi a)^2 \, 2BW_o n_s \tag{14}$$

where T_s = mean time between impulses

n_s = number of impulses per second

In the experimental tests, the carrier frequency deviation and modulating signal bandwidth are small in comparison with the input BW_{IF}. Thus, the total number of impulses occurring per second is associated with a carrier only (no modulation) and can be written (ref. 1)

$$n_s = \frac{BW_{IF}}{2\sqrt{3}} \, erfc \, \sqrt{SNR_{in}} \tag{15}$$

where BW_{IF} = input bandwidth to the demodulator

erfc = complementary error function

SNR_{in} = input SNR to the demodulator

The total impulse power, combining equations (14) and (15), can be written

$$P_{N_s} = \frac{(2\pi a)^2}{\sqrt{3}} \, BW_o BW_{IF} erfc\sqrt{SNR_{in}} \tag{16}$$

Quantization noise is introduced into the output signal by the delta modulator processing technique. This quantization noise is attributable to the error voltage $\epsilon(t)$, or the difference between the sinusoidal input signal $m(t)$ and the delta modulator estimate of the signal $\hat{m}(t)$ (fig. 15). The magnitude of the error signal is always less than the step sizes of the delta modulator, provided the system is not operating under slope overload conditions. The frequency spectrum of the quantization noise is

assumed to be white and continuous from zero to the cut-off frequency of the shaping filter bandwidth BW_s preceding the delta modulator. Because the spectral density of the quantization noise has been determined to be $\dfrac{S_A^2 \tau_{\Delta M}}{6}$ (ref. 2), the quantization noise power is written

$$P_{N_q} = \int_{-BW_o}^{BW_o} G_{N_q}(f)\,df = \int_{-BW_o}^{BW_o} \frac{S_A^2 \tau_{\Delta M}}{6}\,df = \frac{S_A^2}{3}\,\tau_{\Delta M} BW_o \qquad (17)$$

where $G_{N_q}(f)$ = quantization noise spectral density

$\qquad S_A$ = step amplitude of the delta modulator signal estimation

$\qquad \tau_{\Delta M}$ = time period of the delta modulator clock pulse

The SNR_o, as determined from equations (11), (12), (16), and (17) can be written

$$SNR_o = \frac{P_{S_o}}{P_{N_{TH}} + P_{N_s} + P_{N_q}}$$

$$= \frac{\dfrac{a^2 (2\pi)^2 \Delta f^2}{2}}{\dfrac{8\pi^2}{3} \dfrac{a^2 \phi_{IF}}{A^2} BW_o^3 + \dfrac{(2\pi a)^2}{\sqrt{3}} BW_o BW_{IF}\,\mathrm{erfc}\sqrt{SNR_{in}} + \dfrac{S_A^2}{3}\,\tau_{\Delta M} BW_o} \qquad (18)$$

If the SNR_{in} is represented by

$$SNR_{in} = \frac{\dfrac{A^2}{2}}{BW_{IF}\phi_{IF}} \qquad (19)$$

and a reduction factor K is inserted to account for the reduction in impulse noise power due to DM encoding, equation (18) can be rewritten

$$SNR_o = \frac{\frac{3}{2} \Delta f^2 \frac{BW_{IF}}{BW_o^3} SNR_{in}}{1 + K\sqrt{3} \frac{BW_{IF}}{BW_o^2} SNR_{in} \, erfc\sqrt{SNR_{in}} + SNR_{in} \frac{S_A^2}{(2\pi a)^2} \tau_{\Delta M} \frac{BW_{IF}}{BW_o^2}} \qquad (20)$$

When the delta modulator is set to the slope-overload condition, that is, $S_A = \omega_m A_m \tau_{\Delta M}$ where $A_m = 2\pi a \, \Delta f$ (from eq. (11)), then the SNR_o equation becomes

$$SNR_o = \frac{\frac{3}{2} \Delta f^2 \frac{BW_{IF}}{BW_o^3} SNR_{in}}{1 + K\sqrt{3} \frac{BW_{IF}}{BW_o^2} SNR_{in} \, erfc\sqrt{SNR_{in}} + SNR_{in} BW_{IF} \frac{\Delta f^2}{BW_o^2} f_m^2 \tau_{\Delta M}^3 (2\pi)^2} \qquad (21)$$

Equation (21) is descriptive of the FM improvement for the system shown in figure 22 when the modulator is set to the slope-overload condition. The below-threshold SNR improvement, attributable to the encoding of the signal plus noise by the delta modulator, is reflected in the impulse noise reduction factor K. This factor K, which is always less than or equal to unity, is derived in the appendix. The delta modulator does not eliminate impulses; instead, it reduces the noise power associated with each impulse. For channel operation above the FM threshold (where no impulses are present), the K factor does not affect the output SNR.

Computer Simulations of a Basic Delta Modulator

A computer simulation of a delta modulator is used to display graphically the encoding process applied to the demodulated output of an FM system operating below threshold. Shown in figures 23 to 25 are computer-generated plots of the encoding of a sinusoidal signal that has a single threshold noise impulse located in the peak amplitude (zero slope) region of the waveform. In each figure, the encoded delta modulator output is shown superimposed on the analog input. The occurrence of the threshold noise is represented by a rectangular discontinuity in the analog waveform. The step duration is the single variable parameter in each figure; the remaining signal and delta modulator values are held constant. Figure 23 represents a case in which the delta modulator is slope overloading on the portion of the waveform shown in the right-hand side of the figure. The number of steps or levels N_L per impulse duration τ_s is

24

three. The area of the encoded impulse, in terms of delta modulator steps, is proportional to N_L^2 as described in the appendix.

Conditions: $\text{Power}_{\Delta s} \propto 81 S_A^2 \tau_{\Delta M_3}^2$

$\tau_{\Delta M_3}$ = delta modulation step duration

$\tau_{\Delta M_3}$
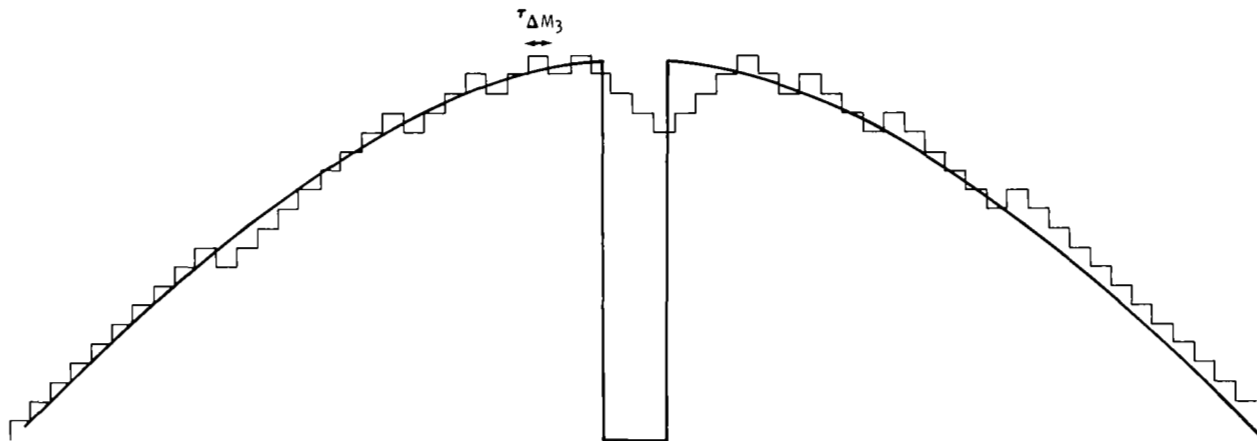
Figure 23. - Simulation of the encoded impulse for a basic delta modulator when $N_L = 3$.

Conditions: $\text{Power}_{\Delta s} \propto 144 S_A^2 \tau_{\Delta M_3}^2$

$\tau_{\Delta M_4} = 0.75 \tau_{\Delta M_3}$

$\tau_{\Delta M_4}$
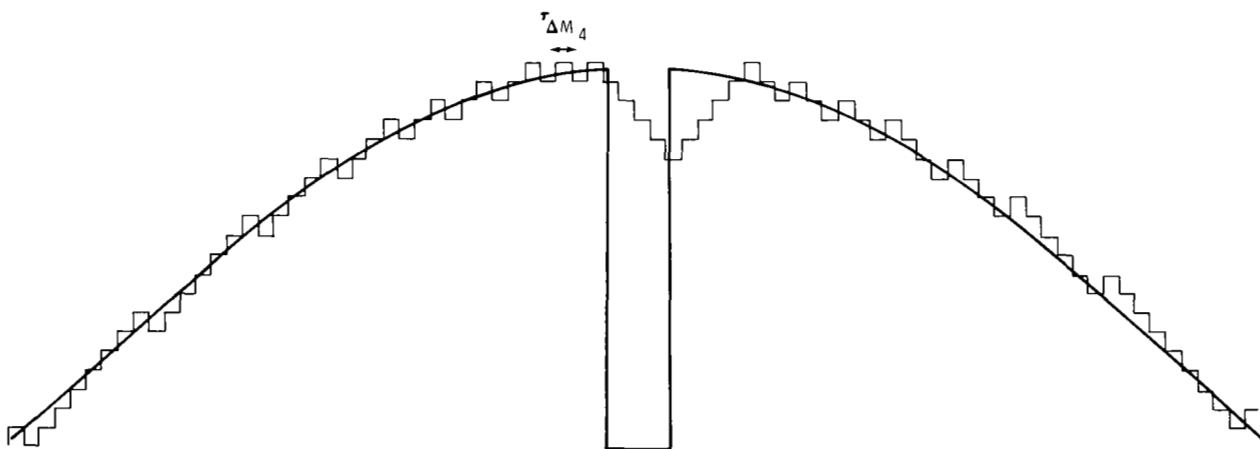
Figure 24. - Simulation of the encoded impulse for a basic delta modulator when $N_L = 4$.
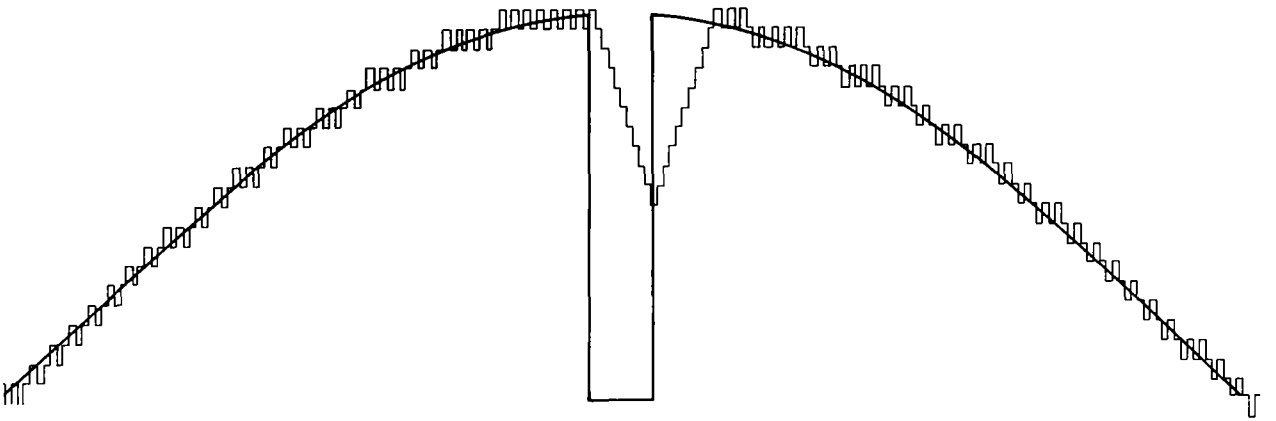
Figure 25.- Simulation of the encoded impulse for the basic delta modulator
when $N_L = 10$.

Figure 24 represents the condition in which $N_L = 4$, and the delta modulator is
not slope overloading. The step duration in figure 24 is $0.75\tau_{\Delta M_3}$, where $\tau_{\Delta M_3}$ is
defined as the step duration in figure 23. The power represented by each encoded noise
impulse is proportional to the area squared, which is shown in the appendix to be equal to

$$\left(\text{Area}_{\Delta s}\right)^2 = N_L{}^4 S_A{}^2 \tau_{\Delta M}{}^2 \tag{22}$$

where S_A is the amplitude of the step and $\tau_{\Delta M}$ is the duration of the delta modulator
pulse. A comparison of the relative power P in the encoded impulses of figures 23
and 24 is obtained from the relationship

$$P_1 \propto \left(N_L{}^2 S_A \tau_{\Delta M_3}\right)^2 = \left(9 S_A \tau_{\Delta M_3}\right)^2 = 81 S_A{}^2 \tau_{\Delta M_3}{}^2 \tag{23}$$

where $N_L = 3$, and

$$P_2 \propto \left(N_L{}^2 S_A \tau_{\Delta M_4}\right)^2 = \left(16 S_A 0.75 \tau_{\Delta M_3}\right)^2 = 144 S_A{}^2 \tau_{\Delta M_3}{}^2 \tag{24}$$

26

where $N_L = 4$. The encoded impulse in figure 24 exceeds the power contained in the encoded impulse of figure 23 by a factor of 1.78. Thus, as the delta modulator step duration $\tau_{\Delta M}$ decreases, the relative power in the encoded impulse increases. This relationship is to be expected, because decreasing the delta modulator step duration improves the resolution of the encoded waveform and increases the frequency response of the system. Thus, as $\tau_{\Delta M}$ is reduced, the encoded estimate of the noise impulse improves, and the power of the encoded impulse approaches that of the input data. In the limit, as $\tau_{\Delta M} \rightarrow 0$, the area of the encoded impulse $\text{Area}_{\Delta s}$ approaches that of the uncoded impulse Area_s or

$$\text{Area}_{\Delta s} \rightarrow \text{Area}_s \qquad (25)$$

The increase in size and relative amplitude of the encoded impulse, as $\tau_{\Delta M}$ is further reduced, is shown in figure 25 for $N_L = 10$.

Interpolating Delta Modulator

The threshold extension performance of the basic delta modulator is limited by the catchup phenomenon that determines the minimum obtainable encoded impulse area $\text{Area}_{\Delta s}$. However, a modification to the basic delta modulation system can reduce substantially the minimum obtainable area of the encoded impulse by eliminating the catchup phenomenon.

A block diagram of the modified system, designated the interpolating delta modulator (IDM), is given in figure 26. The IDM is identical to the basic delta modulator shown in figure 15 except that an integrator disable line is added, and a level detector pair is incorporated into the differential comparator. The following operations of the IDM are different from those of the basic device.

1. The differential comparator in the IDM detects the polarity and the magnitude of the difference between the analog signal input $m(t)$ and the encoded estimate $\hat{m}(t)$.

2. If the magnitude of $m(t) - \hat{m}(t)$ exceeds a predetermined reference level, a disable pulse is generated.

3. The disable pulse gates the integrator OFF.

4. The duration of the disable pulse is approximately equal to the duration of a threshold noise impulse τ_s.

5. The encoded output of the delta modulator during a noise impulse is an alternating (positive-negative) step sequence.
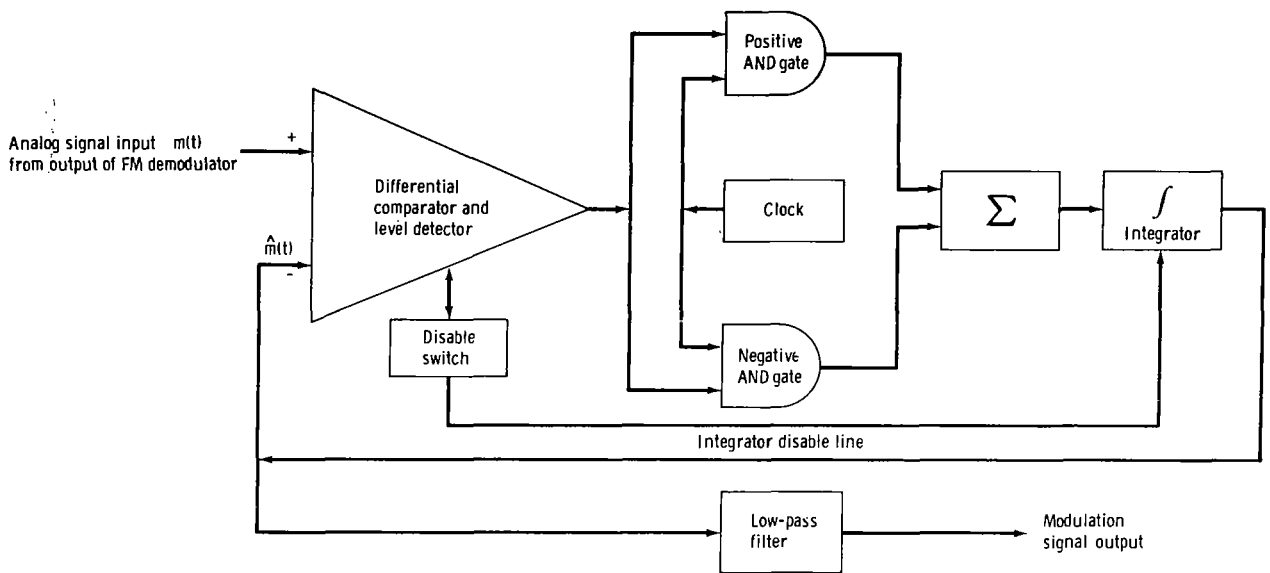
Figure 26. - The IDM threshold extension system.

The result is that the output of the IDM coasts across each noise impulse instead of encoding each impulse. The effective area of the noise impulse is drastically reduced, thereby reducing noise power.

A computer-generated plot simulating the encoding of a sinusoidal signal that has a single noise impulse located in the peak amplitude region of the waveform is shown in figure 27. The step amplitude S_A and duration $\tau_{\Delta M}$ are identical to those used in figure 23.

The number of unit areas represented by the interpolation of a noise impulse is $N_L/2$, whereas the number of unit areas represented by the encoded noise waveform for
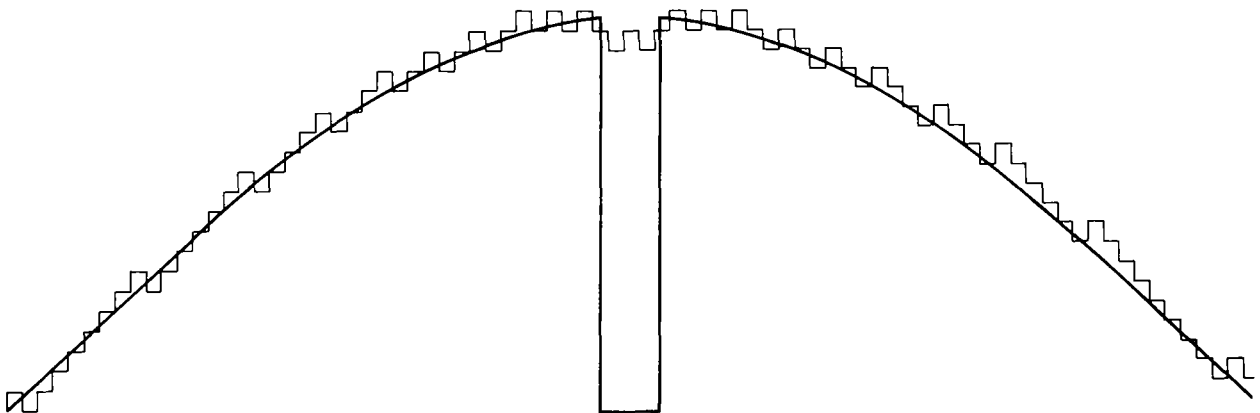
Figure 27. - Simulation of the encoded impulse for the IDM when $N_L = 4$.

28

the basic delta modulator is N_L^2 as described in the appendix. Therefore, compared with the basic delta modulator system, the IDM provides an area reduction factor of $1/2N_L$.

The noise power reduction factors $K_{\Delta M}$ and K_{IDM} for the basic delta modulator and IDM systems, respectively, are written in the appendix

$$K_{\Delta M} = \frac{N_L^2 S_A \tau_{\Delta M}}{2\pi a} \tag{26}$$

$$K_{IDM} = \frac{\frac{N_L}{2} S_A \tau_{\Delta M}}{2\pi a} \tag{27}$$

When the performance of the IDM system is compared with that of the basic delta modulator operating under the optimum conditions (slope overload) as shown in figure 24, the reduction in impulse noise power of the IDM system is

$$P_{N_S} \text{ reduction} \propto \left(\frac{1}{2N_L}\right)^2 = \frac{1}{64} \tag{28}$$

where $N_L = 4$ encoding levels.

With the IDM system, the power of the encoded impulse is at a minimum when the system is operating at slope overload. A reduction in step duration, while holding the step amplitude S_A constant, does not reduce encoded noise power as might be implied from equation (27). This relationship can be shown by considering two IDM systems in which N_L is equal to 4 and 10, respectively, and S_A is adjusted for slope overload only for the $N_L = 4$ condition.

If K_{IDM4} and K_{IDM10} represent the reduction factors for the IDM systems in which N_L is equal to 4 and 10, respectively, the equation can be written

$$\frac{K_{IDM4}}{K_{IDM10}} = \frac{\frac{\frac{4}{2} S_A \tau_{\Delta M4}}{2\pi a}}{\frac{\frac{10}{2} S_A \tau_{\Delta M10}}{2\pi a}} = \frac{4\tau_{\Delta M4}}{10\tau_{\Delta M10}} \tag{29}$$

Because $\tau_{\Delta M4} = (10/4)\tau_{\Delta M10}$, equation (29) reduces to

$$K_{IDM4} = K_{IDM10} \qquad (30)$$

Thus, for an IDM system, the encoded noise power is always equal to the power corresponding to the slope overload condition. Decreasing the step duration will not change the amount of impulse power.

However, the IDM system has one significant difference from the basic DM system. It can be shown from equation (26) that the encoded impulse power for the basic delta modulator is the same for all slope overload conditions. That is, as long as the ratio $S_A/\tau_{\Delta M}$ remains equal to the slope overload condition, the particular values of S_A and $\tau_{\Delta M}$ are irrelevant. However, for the IDM system (eq. (27)), reducing the S_A and $\tau_{\Delta M}$, while keeping the ratio $S_A/\tau_{\Delta M}$ constant, reduces the encoded noise power. Therefore, the overall threshold extension performance of the IDM can be improved by decreasing the step duration until the bandwidth constraints of the system become the limiting factor.

The analysis of the delta modulator has been limited primarily to the condition in which a noise impulse occurs at a point of zero slope on the signal waveform. However, it is possible for impulses to occur along the region of maximum slope of the signal waveform. Under this condition, the area of the encoded impulses will not be the same as that obtained at zero slope. Using the basic delta modulator, the encoded area for an impulse on a maximum slope region will be less than the case for zero slope, if the polarity of the noise impulse is the same as the signal waveform slope polarity. If the impulse noise polarity is opposite the signal waveform slope polarity, the encoded impulse noise area will be greater than that at zero slope. For the latter condition, the noise contribution due to the catchup phenomenon can be reduced significantly by using the IDM. Figures 28 and 29 represent the performance of the basic delta modulator and
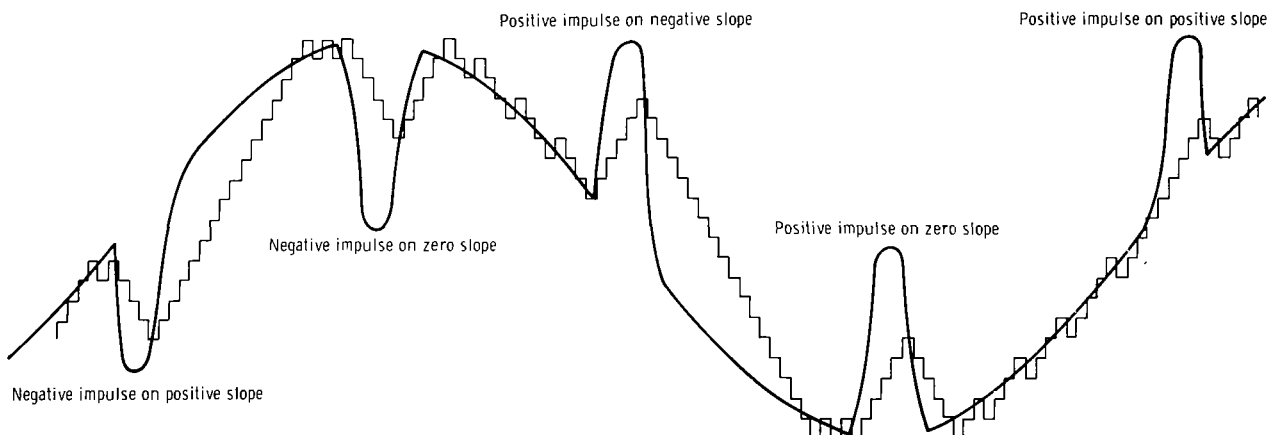

Figure 28.- The effects of signal slope on the encoded waveform, using the basic delta modulator.
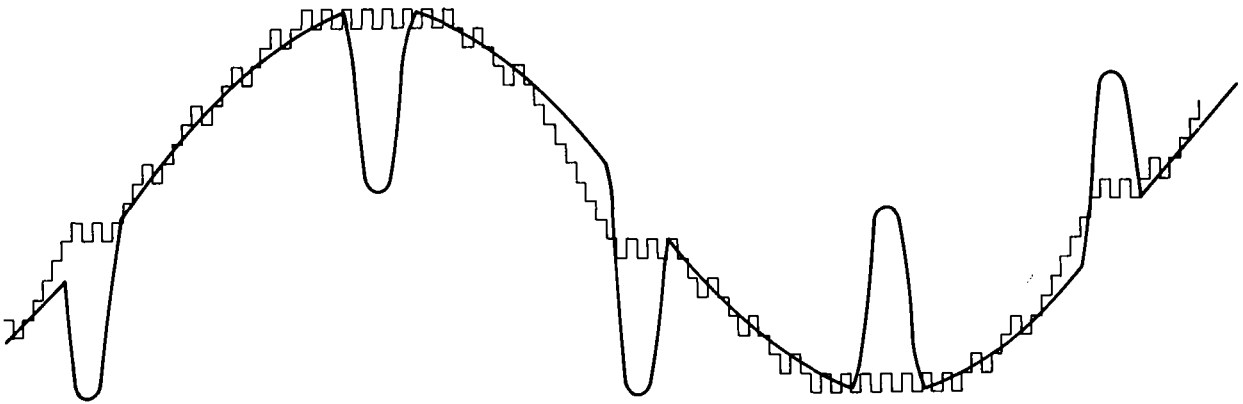
Figure 29. - The effects of signal slope on the encoded waveform with the IDM.

the IDM, respectively, when noise impulses occur on both the positive and negative slope regions of the signal waveform.

EXPERIMENTAL RESULTS

The performance of the various threshold extension techniques can be evaluated in terms of the capability of each device to improve the output signal of a PLL FM demodulator. In particular, a qualitative estimate of the signal enhancement is obtained by comparing the demodulated signal waveforms and noise spectrum at the input and output of the threshold extension devices. A quantitative estimate of the signal enhancement is obtained from SNR tests that indicate the output SNR improvement and the amount of realizable threshold extension. The results of bit error rate (BER) tests also are used to evaluate the effectiveness of the threshold extension techniques.

Experimental results are presented in the following paragraphs for the basic impulse noise eliminator, the correlation detection technique, and the DM technique.

Waveform Analysis

The improvement in the quality of a demodulated signal through the use of a threshold extension system can be demonstrated by comparing the input and output waveforms of the device. The basic system configuration for the waveform analysis tests is shown in figure 30. The test configuration enables simultaneous operation of the delta modulator and the impulse noise eliminator so the combined improvement and the individual performance of these devices can be determined.
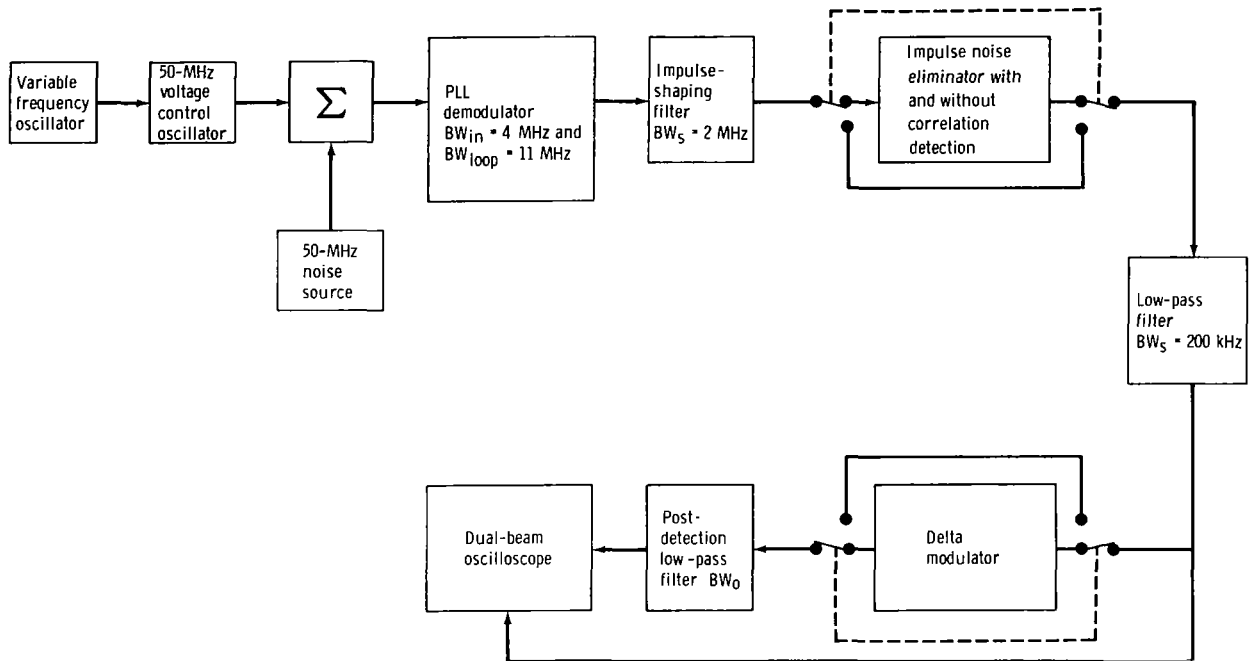
Figure 30.- Basic system configuration for waveform analysis tests.

Impulse noise eliminator. - The effect of the impulse noise eliminator on the signal-plus-noise waveforms is shown in figures 31, 32, and 33. The upper waveform in each photograph represents the postdetection filter output of a PLL FM demodulator operating below threshold without the benefit of impulse noise elimination. The lower
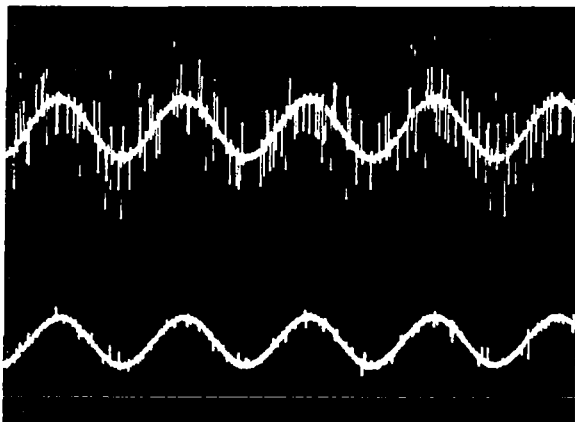
Figure 31.- Demodulated 1-kilohertz sine wave plus impulse noise. The upper trace is without impulse noise elimination; the lower trace is with the basic impulse noise eliminator.
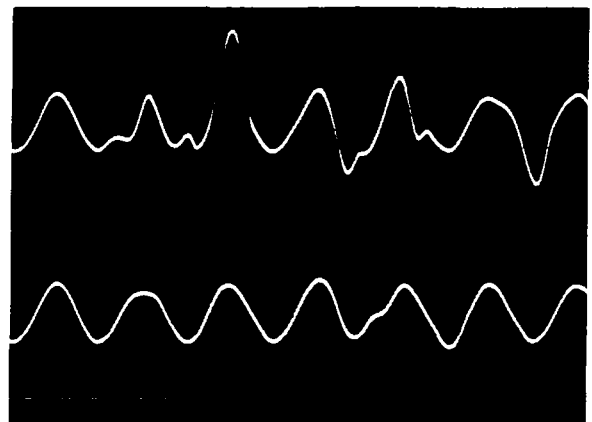
Figure 32.- Demodulated 30-kilohertz sine wave plus impulse noise. The upper trace is without impulse noise elimination; the lower trace is with a basic impulse noise eliminator.

Figure 33. - Demodulated 10-kilohertz square wave plus impulse noise. The upper trace is without impulse noise elimination; the lower trace is with a basic impulse noise eliminator.

trace in each figure represents the effect of impulse noise elimination on the demodulated signal prior to postdetection filtering.

A situation in which the modulation frequency is low compared with the impulse duration is represented in figure 31. A demodulated 1-kilohertz sine wave is shown punctuated with noi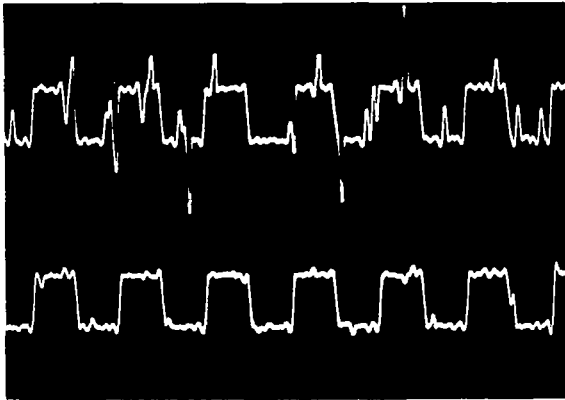se impulses that have a duration of approximately 10 microseconds. The sinusoidal shape of the waveform is not altered significantly by the amplitude excursion of a single impulse. However, the noise contribution of the impulses shown in the upper trace of figure 31 is considerable (10 decibels) because of the number of impulses. The lower trace indicates that the impulse noise eliminator is successful in eliminating most of the impulse noise from the demodulated waveform.

A situation in which the impulse duration approaches the modulation frequency is represented in figure 32. A single noise spike will cause considerable distortion to the shape of the demodulated signal waveform. The distortion is illustrated by the upper trace (fig. 32), which represents noise impulses that have a duration of 10 milliseconds on a demodulated 30-kilohertz sine wave. The lower trace demonstrates the capability of the basic impulse noise eliminator to provide a modulation estimate as a substitute for the distortion caused by the occurrence of noise spikes on the demodulated signal. The SNR improvement and degree of threshold extension are the same as those obtained for figure 31.

A simulated digital signal, represented by a 10-kilohertz square wave is shown in figure 33. The waveform improvement is similar to that obtained with the sinusoidal signals.

Correlation detection. - The modified impulse noise eliminator produced significant improvements in the signal waveforms when the correlation detection technique, as represented in figure 34, is used. However, the primary advantage of the correlation detection technique is that the range of frequency deviations that can be processed by the impulse noise eliminator is increased considerably. This technique is especially useful with FM channels in which the basic impulse noise eliminator level detectors cannot be adjusted to detect threshold noise impulses without also detecting the peaks of the modulating waveform.

The waveform improvement that is obtained when the correlation detection technique is used is shown in figures 34 and 35. A 1-kilohertz modulation waveform with a 1-megahertz peak frequency deviation at the output of an FM demodulator through a 500-kilohertz low-pass postdetection filter is shown in figure 34. The fact that the demodulator is operating below threshold is indicated by the number of noise impulses. However, the amplitude of the noise impulse is only approximately one-fourth of the
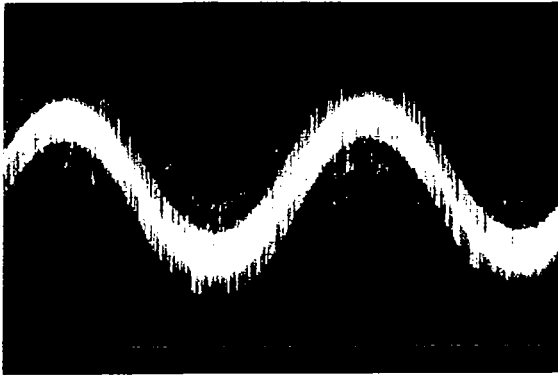
Figure 34. - Signal-plus-noise output for
a large frequency deviation without
correlation detection. Conditions:
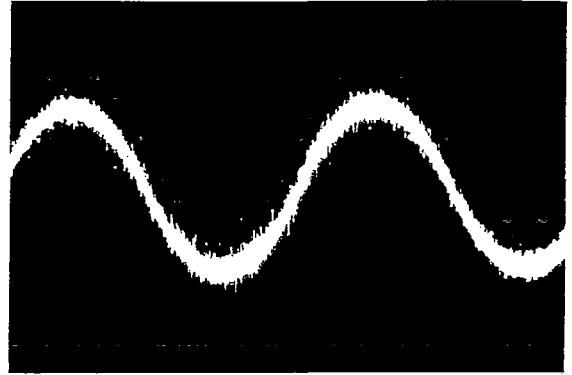f_m = 1 kHz, BW_o = 500 kHz,
Δf = 1 MHz.

Figure 35. - Impulse noise elimination
obtained by using correlation detec-
tion. Conditions: f_m = 1 kHz,
BW_o = 500 kHz, Δf = 1 MHz.

total signal amplitude, which is a result of the large frequency deviation. The basic impulse noise eliminator cannot be adjusted to detect the noise impulses without severely clipping the signal in the process. The use of correlation detection, however, permits the noise elimination process to be accomplished without any undesirable degradation to the signal waveform.

Delta modulation. - The DM encoding of the output signal plus noise results in similar improvements in the output waveforms. The waveform in figure 36 represents the signal-plus-noise output of the FM demodulator without the DM threshold extension device. A 60-kilohertz low-pass postdetection filter is used in this test configuration.

Figure 37 represents the encoded sig-
nal plus noise shown in figure 36. The delta
modulator step amplitude is 0.025 volt, and
the step duration is 20 microseconds. The
effective output bandwidth of the delta mod-
ulator is approximately 5 kilohertz. All of
the noise impulses have been suppressed by
the encoding process of the delta modulator.

Investigations were made to ensure
that the DM encoding process did not intro-
duce spurious noise frequencies into the
signal spectrum. Photographs of the signal-
plus-noise spectrum before and after proc-
essing are shown in figures 38 and 39. A
10-kilohertz signal is represented by the
large amplitude spike. The total noise spec-
trum can be observed extending along the
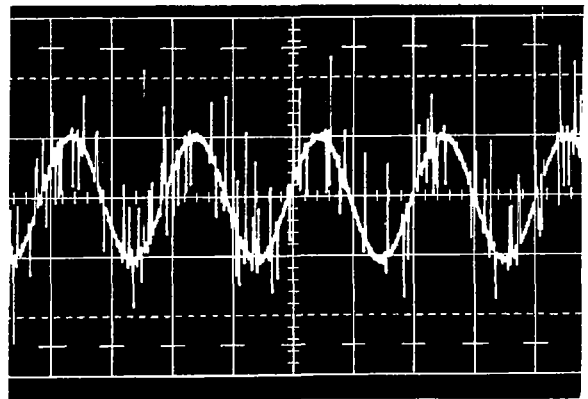length of the figure, which has a scale of
10 kHz/cm.

Figure 36. - Signal-plus-noise output
without a DM system. Conditions:
f_m = 1 kHz, Δf = 100 kHz,
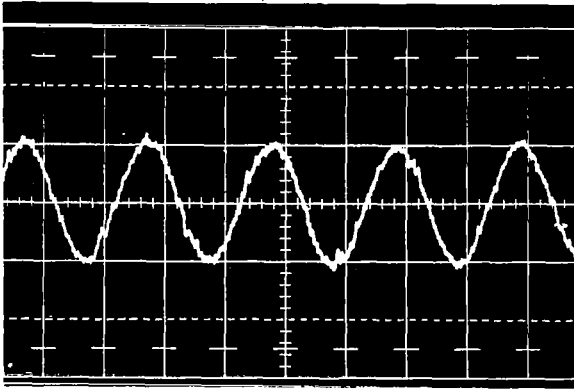BW_o = 60 kHz.

34

Figure 37. - Encoded signal-plus-noise output with a DM system. Conditions: $f_m = 1$ kHz, $\Delta f = 100$ kHz, $BW_0 = 60$ kHz.
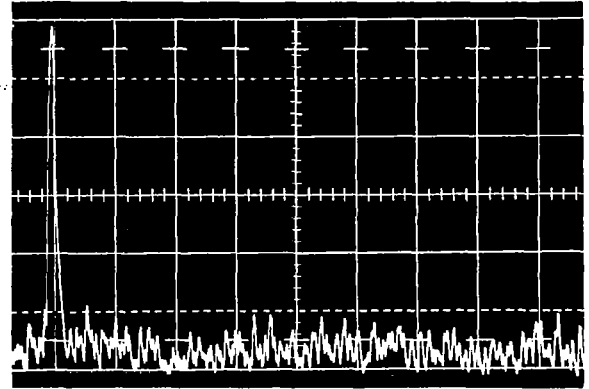
Grid interval = 10 kHz

Figure 38. - Demodulator output signal-plus-noise spectrum without a DM system. Conditions: $f_m = 10$ kHz and $SNR_{in} = 2$ dB.
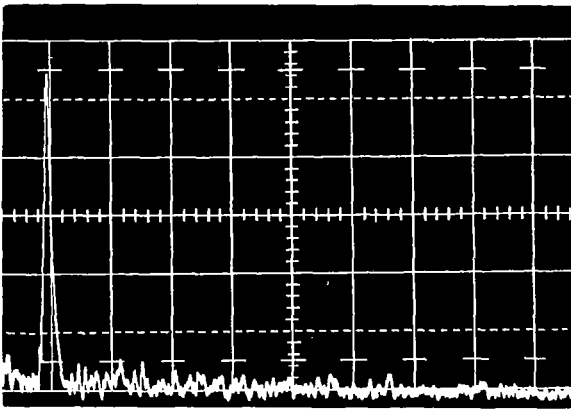
Grid interval = 10 kHz

Figure 39. - Demodulator output signal-plus-noise spectrum with a DM system. Conditions: $f_m = 10$ kHz and $SNR_{in} = 2$ dB.

The demodulator output signal-plus-noise spectrum, obtained when using the delta modulator, is shown in figure 39. No new spurious noise components are observed. A significant decrease in the amplitude of the noise spectral components also is noted. The reduction in noise around the 10-kilohertz test tone can be attributed directly to the delta modulator signal processing. However, the tapering amplitude of the noise spectral components for the remainder of the photograph is primarily a result of the decreased frequency response attributable to the delta modulation processing.

Signal-to-Noise-Ratio Tests

A quantitative estimate of the performance improvement due to the threshold extension techniques may be obtained from the results of SNR tests conducted in the MSC Signal Design Verification Laboratory. The purposes of the SNR tests are

1. To determine the noise reduction and threshold extension capabilities of the impulse noise eliminator (with and without signal-correlation detection) and the delta modulator

2. To obtain base-line measured data to verify the theoretical analysis

35

A block diagram of the SNR test configuration that is used to obtain data for a single channel FM system is shown in figure 40. Series or individual operation of the delta modulator and the impulse noise eliminator (with and without correlation detection) is possible with the test configuration. The output noise power measurements were made while the modulating signal was disabled so that a comparison could be made with the test data and the theoretical results.
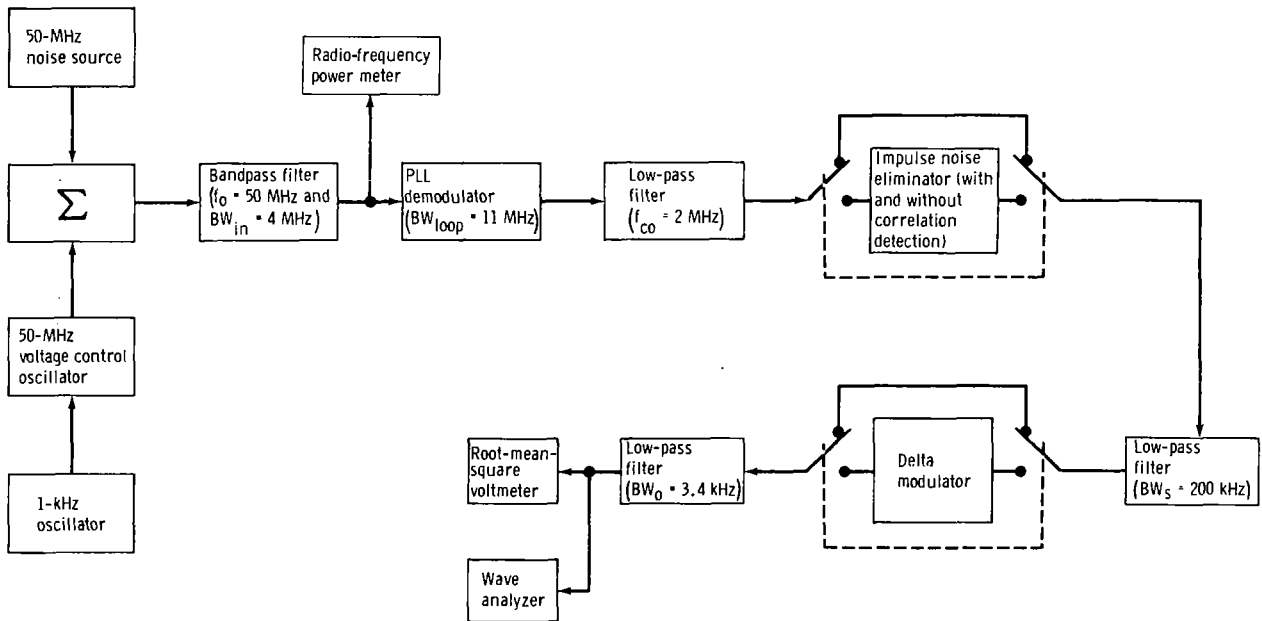
50-MHz noise source

Radio-frequency power meter

Σ

Bandpass filter ($f_0 = 50$ MHz and $BW_{in} = 4$ MHz)

PLL demodulator ($BW_{loop} = 11$ MHz)

Low-pass filter ($f_{co} = 2$ MHz)

Impulse noise eliminator (with and without correlation detection)

50-MHz voltage control oscillator

1-kHz oscillator

Root-mean-square voltmeter

Low-pass filter ($BW_0 = 3.4$ kHz)

Delta modulator

Low-pass filter ($BW_S = 200$ kHz)

Wave analyzer

Figure 40. – Single channel FM threshold extension SNR test configuration.

The SNR improvement and threshold extension obtained with the basic impulse noise eliminator and the delta modulator implemented at the output of a PLL demodulator are shown in figure 41. The impulse noise eliminator provides a 2.5-decibel maximum threshold extension and a 12-decibel maximum improvement in output SNR. A threshold extension of approximately 1.5 decibels is obtained by using the delta modulator. A maximum impulse noise power reduction of approximately 7 decibels is reflected by the corresponding output SNR improvement for a given input level. The basic impulse noise eliminator and delta modulator operating in series with the demodulator output give a 3-decibel combined input SNR improvement below threshold.

Measured data for an IDM are not available. However, the performance of the interpolating device should be comparable to that of the basic impulse noise eliminator.

The performance of the correlation detection technique implemented at the output of a single-channel FM system is shown in figure 42. The test configuration is similar to that represented in figure 40, except that the delta modulator is bypassed and the peak frequency deviation is increased to approximately 160 kilohertz. The test results indicate that the performance improvement of the basic impulse noise eliminator is
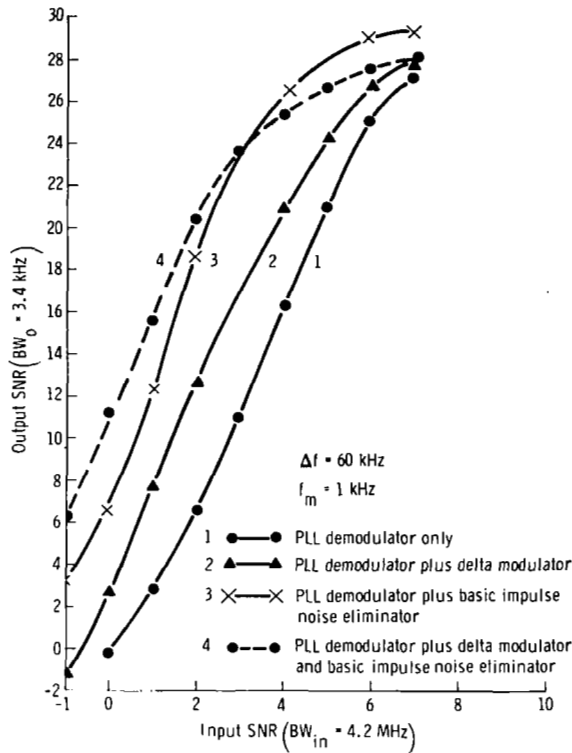
Figure 41. - Single channel SNR performance of threshold extension devices.

Figure 42. - Correlation detection SNR tests.

similar to that of the correlation detection/ impulse noise eliminator. The basic device provides approximately 2 decibels of threshold extension, and the correlation detection system provides slightly less than 2 decibels of threshold improvement.

The performance of the threshold extension techniques also was analyzed using an FM/FM system. The basic test configuration for these tests consisted of two FM demodulators connected in tandem. For the first set of tests, the threshold extension devices were inserted between the output of the first demodulator and the input to the second demodulator; later, the extension devices were inserted after the second demodulator only. The carrier frequency deviation Δf_1 and subcarrier frequency deviation Δf_2 are selected such that both demodulators experience threshold operation at the same input SNR value. Thus, if threshold noise impulses are present in the output of the carrier frequency demodulator, noise impulses also will be present in the output of the

subcarrier demodulator. The purpose of the first configuration was to determine what effect the elimination of noise impulses at the output of the carrier frequency demodulator would have on the threshold performance of the subcarrier demodulator. Test results indicate that a threshold extension of less than 0.3 decibel can be obtained by using the first configuration.

For the second configuration in which the threshold device was placed at the output of the second FM demodulator, a maximum extension of 1 decibel is achieved below FM threshold. The results obtained by using the correlation detection/impulse noise eliminator in the second configuration are shown in figure 43. The failure to obtain significant threshold extension with the FM/FM configurations may be attributed to the complex interrelationships between threshold noise in the output of the carrier frequency demodulator and the threshold performance of the second demodulator rather than to a lack of performance on the part of the threshold extension devices (ref. 2).
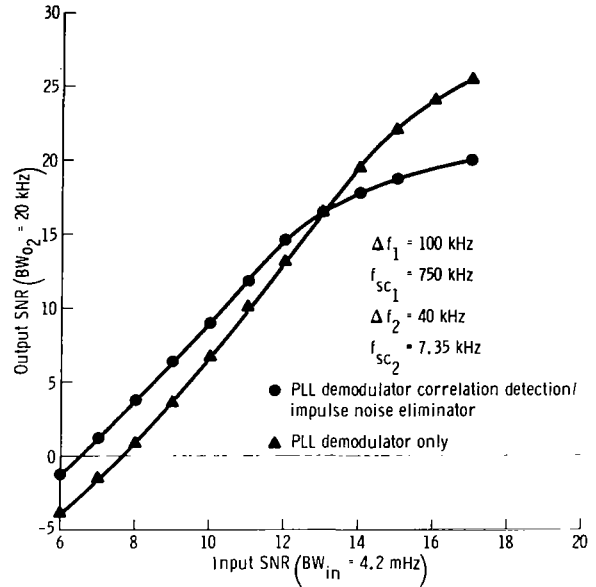
Figure 43. – The FM/FM correlation detection SNR tests.

Bit Error Rate Tests

A series of BER tests was conducted to determine the performance of the threshold extension techniques when used to process digital information. The BER data were obtained by using the test configuration shown in figure 44.

The test data in figure 45 represent the BER performance as a function of the SNR into a PLL demodulator with and without the basic impulse noise eliminator. A bit rate of 51.2 kbps was used to modulate the 50-megahertz voltage control oscillator with a peak frequency deviation of 100 kilohertz. A 2-decibel threshold extension is obtained for 51.2-kbps telemetry data for a 10^{-6} BER when the basic impulse noise elimination technique is used.

A similar BER test was conducted in the MSC Electronic Systems Compatibility Laboratory by using actual Apollo spacecraft hardware and a calibrated radio-frequency path. The curves presented in figures 45 and 46 cannot be compared directly because of test-configuration differences in input bandwidth and demodulator performance. However, the data can be used to determine the relative threshold improvement obtained in each case. A threshold improvement of approximately 6 decibels is obtained by using the test data corresponding to a 10^{-3} BER (fig. 46). The difference in threshold improvement between the two tests is due to the relative demodulator performance, the different predetection and postdetection filtering, and the bit synchronizer performance for each test configuration.
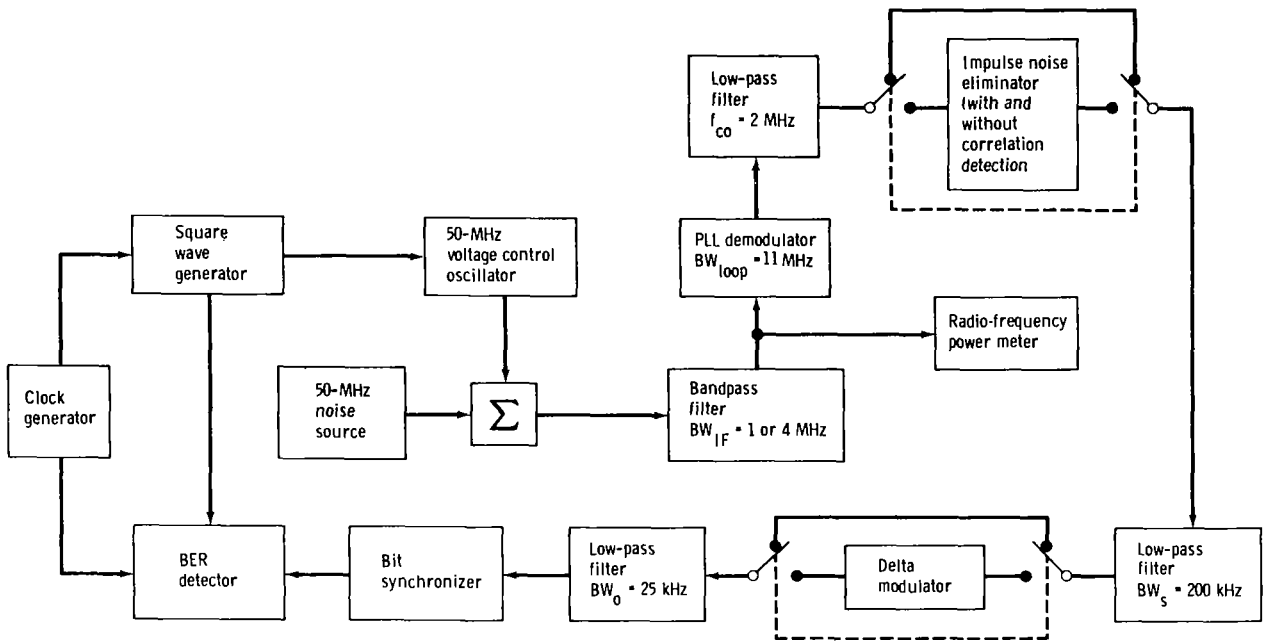
Figure 44. - The BER test configuration for a PLL demodulator.

The data obtained from the BER test using the correlation detection technique are shown in figure 47. A 2-decibel improvement in base-band telemetry (1.6 kbps) is achieved at a 10^{-3} BER.

The performance of a 1.6-kbps data channel, with and without a delta modulator threshold extension device, is shown in figure 48. A bit rate of 1.6 kbps and a peak frequency deviation of 100 kilohertz are used for the tests. A 2-decibel threshold extension is obtained by using the delta modulator at the output of a PLL demodulator.

Figure 45. - The BER performance using the basic impulse noise eliminator and standard laboratory equipment.

Figure 46. - The BER performance using the basic impulse noise eliminator and actual spacecraft equipment.

40

Figure 47. – The BER performance using the correlation detection technique.

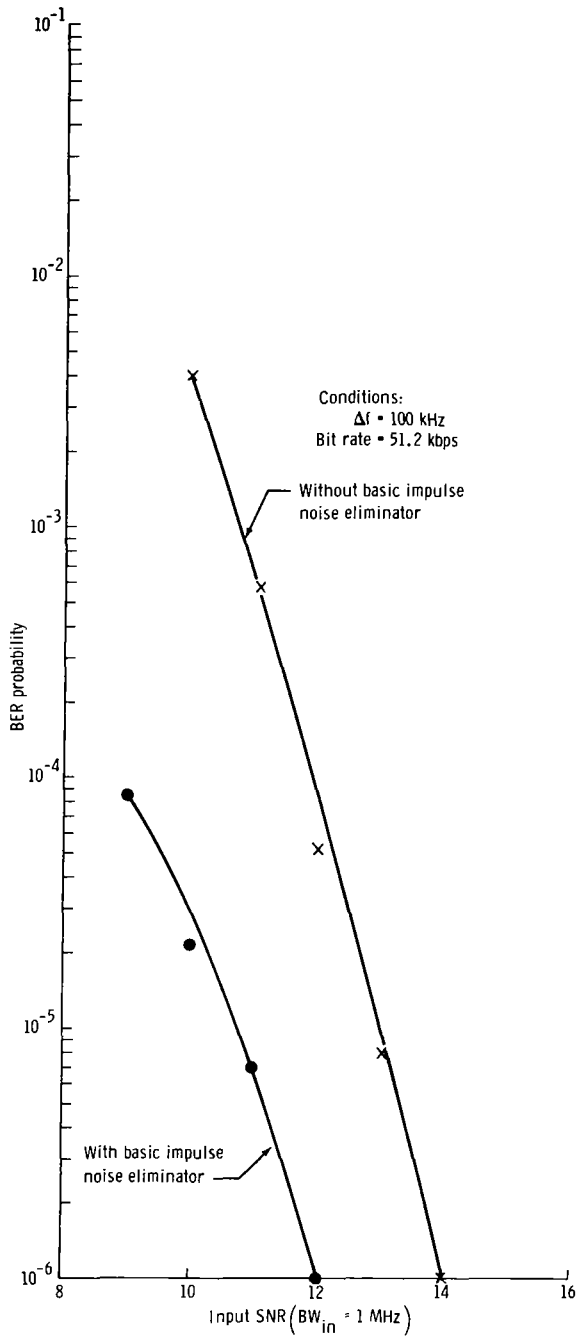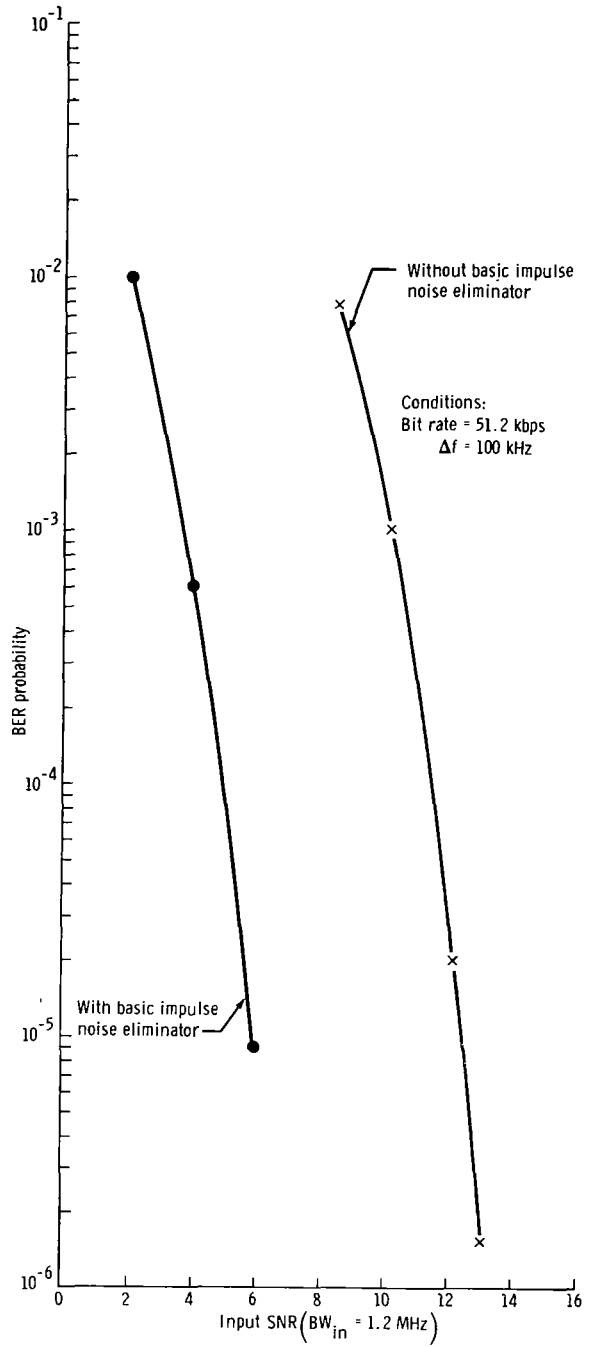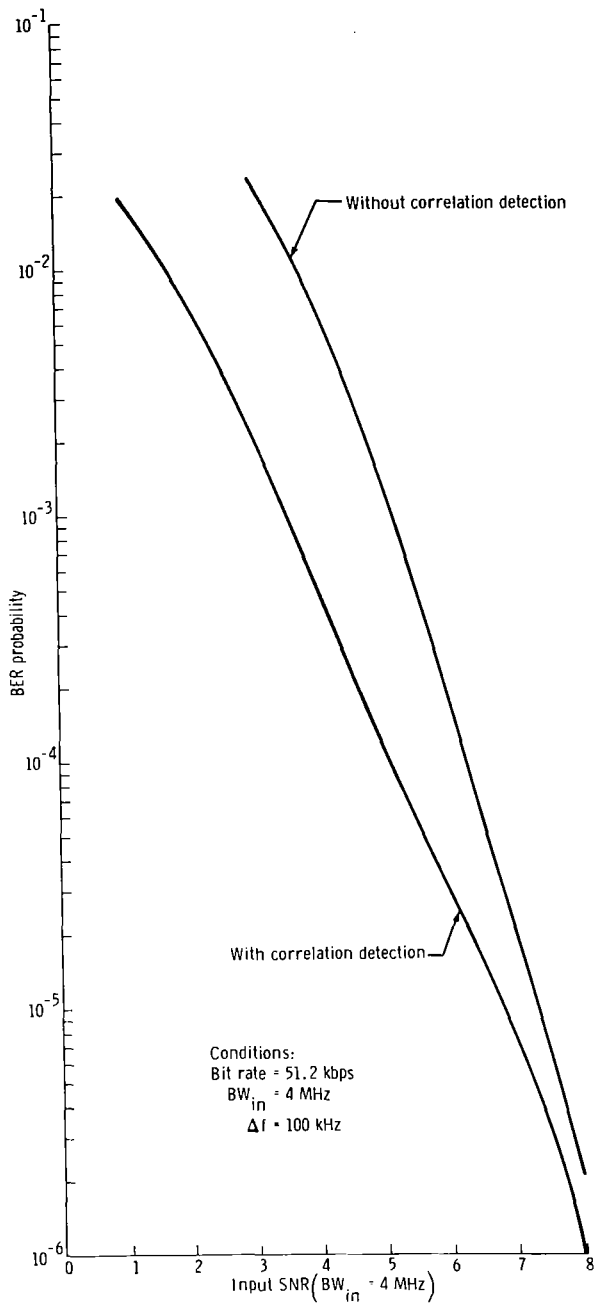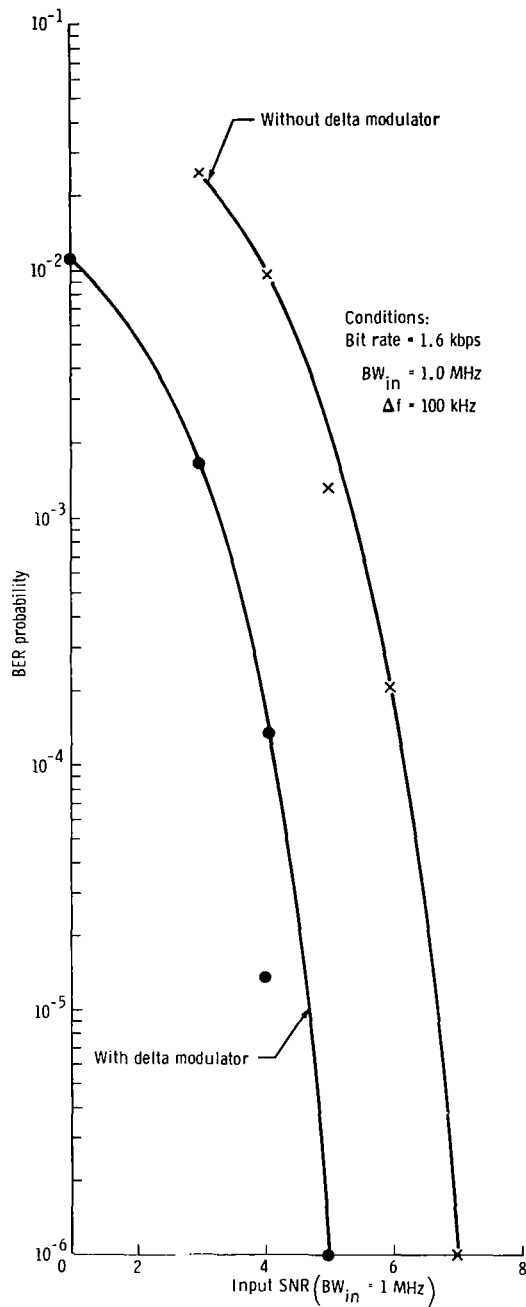Figure 48. – The BER performance using the delta modulator.

41

COMPARISON OF THEORETICAL AND EXPERIMENTAL RESULTS
FOR THE DELTA MODULATOR

A comparison of the experimental and theoretical results for SNR improvement may be used to determine the validity of the mathematical model for the delta modulator (eq. (21)) and, in particular, the accuracy of the calculated factor K (eq. (A11)). The SNR improvement is defined as the difference in output SNR with and without the insertion of the delta modulator after the PLL demodulator. Experimental and theoretical results are compared in figure 49.

When the input SNR is high (above FM threshold), no SNR improvement through the delta modulator occurs because no noise impulses are present in the output of the demodulator. The quantizing noise from the delta modulator sets an upper bound to the maximum achievable output SNR and can degrade performance above FM threshold. However, the quantization noise is small for the particular test configuration and does not degrade the measurable performance. In figure 41, the maximum output SNR is limited to approximately 27 decibels both with and without the use of the delta modulator. The measurements are indicative that noise from the input voltage control oscillator (radio-frequency modulator) rather than quantization noise determines the maximum obtainable output SNR. Therefore, a maximum transmitted SNR of 27 decibels has been included in the theoretical predictions in figure 49 (ref. 3).
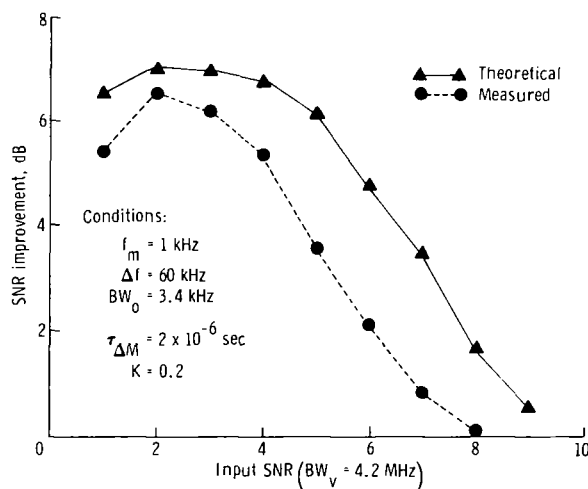
Figure 49. - Comparison of theoretical and experimental results for SNR improvement using the delta modulator.

The theoretical and experimental data compare favorably, which indicates the calculations for the noise reduction factor K are valid. Differences in the SNR curves are due to the occurrence of impulses at times other than at the peaks of the modulation waveform. Most, but not all, of the impulses occur at the modulation peaks (ref. 2). In the derivation of the factor K, the coded and the uncoded noise impulses are considered to occur at the modulation peaks.

CONCLUSIONS

The characteristics of several threshold extension devices have been analyzed with respect to the capability of each device to improve the performance of a phase lock loop demodulator. The results of qualitative waveform analysis tests and quantitative signal-to-noise-ratio and bit error rate tests are used to evaluate the performance of each threshold extension device.

The techniques discussed in this report include a basic impulse noise elimination system, a signal correlation system for detecting impulse noise, and a delta modulation threshold extension device. These devices, utilizing postdetection signal-plus-noise processing techniques, can be implemented in conjunction with any FM demodulator to provide improved system performance.

The results of signal-to-noise-ratio tests indicate that a threshold extension of 2 to 2.5 decibels is consistently obtainable by using either the basic impulse noise elimination technique or the modified system incorporating correlation detection of impulse noise. The signal-to-noise-ratio test data also are indicative that the delta modulation signal processing technique used at the output of a phase lock loop demodulator provides approximately 1.5 decibels of threshold extension. A conceptual interpolating delta modulator, which provides significantly improved threshold extension capability, is discussed and analyzed. The interpolating delta modulator and the impulse noise eliminator provide approximately equivalent theoretical threshold extension performance for a given FM system configuration.

The results of bit error rate tests are indicative that both the impulse noise eliminator and delta modulator threshold extension devices provide similar performance improvement. The measured threshold extension obtained with these devices varied from 2 to 6 decibels. The wide variation in obtainable threshold extension is attributed to the characteristics and adjustment of the particular bit synchronizers used in the test configurations.

The combined results of the signal-to-noise-ratio and bit error rate tests indicate that the impulse noise elimination technique incorporating either correlation detection or delta modulation signal processing can be used at the output of an FM demodulator to provide improved signal-to-noise-ratio and threshold performance. For cases in which these techniques are implemented with a threshold extension demodulator, such as a phase lock loop or frequency modulation feedback demodulator, the improvement provided by the external threshold extension device is in addition to that improvement usually provided by the demodulator alone. Each of the techniques has particular advantages and disadvantages. These may be summarized as follows.

1. Basic impulse noise eliminator. This technique provides the greatest amount of threshold extension by eliminating most of the threshold noise impulses in the demodulator output. However, the basic impulse noise eliminator is limited to signals that have relatively small frequency deviations, because operation of the device requires that the amplitude of each noise impulse must be greater than the peak signal amplitude. As the frequency deviation is increased, the amplitude of the output signal increases correspondingly such that a limiting frequency deviation exists for detecting impulses. Disadvantages of the basic impulse noise eliminator are the complexity and sensitivity to adjustment of the device. The amplitude detectors must be adjusted precisely to the optimum level in order to obtain maximum threshold extension.

2. Correlation detection combined with the basic impulse noise elimination system. With this system, the operating range of the basic impulse noise eliminator is increased considerably with respect to the maximum signal frequency deviations that can be used. This increase results from the relative insensitivity of the system to the amplitude of the demodulated signal. In terms of threshold extension, the performance of the correlation detection system is virtually identical to that of the basic impulse

noise eliminator. The selection of proper time delays in the correlation detectors is critical. However, the correlation detector/impulse noise eliminator combination is considerably less critical to adjust, with respect to the level detectors, than is the basic impulse noise eliminator.

3. Basic delta modulator. This signal-processing technique is the simplest of the threshold extension devices investigated. However, the threshold performance of the basic delta modulator is degraded from that of the basic impulse noise eliminator. A modified delta modulator, which is called an interpolating delta modulator, should provide performance that is equivalent to the impulse noise eliminator. The delta modulator and interpolating delta modulator systems are considered the most practical of the three threshold extension devices that were tested, because of the simplicity and ease of operation. The required adjustments for the delta modulator are few and are less critical than those of the impulse noise eliminator. It is possible that more sophisticated delta modulators could provide greater realizable threshold extension. The interpolating delta modulator is one such device that could be used to achieve greater performance without sacrificing simplicity and ease of implementation.

In conclusion, each of the three threshold extension devices has application in FM systems that operate at low-input signal-to-noise conditions. The characteristics of the modulating signal must be considered in determining which extension technique is best suited for a particular FM channel.

Manned Spacecraft Center
National Aeronautics and Space Administration
Houston, Texas, October 5, 1971
914-50-50-17-72

APPENDIX

DETERMINATION OF THE IMPULSE NOISE REDUCTION FACTOR

The delta modulator encoding technique achieves FM threshold extension by reducing the noise power associated with each impulse rather than by eliminating the impulses present in the signal. The reduction in noise power is accomplished by reducing the area of the impulse waveform. The factor K in the SNR improvement equation (eq. (21)) is a measure of the amount of reduction in impulse area. Specifically, K is a ratio of the encoded noise area to the uncoded area and is given by

$$\sqrt{K} = \frac{\text{Area}_{\Delta s}}{\text{Area}_s} \tag{A1}$$

where $\text{Area}_{\Delta s}$ = area of the delta modulator encoded impulse

Area_s = area of the uncoded impulse

The factor K has several properties of interest.

1. $K \leq 1$. Delta modulation always should improve FM threshold performance, with a proper selection of modulator parameters.

2. $K \rightarrow 1$ as $\tau_{\Delta M} \rightarrow 0$. As the pulse width of the basic delta modulator approaches zero, the area of the coded impulse approaches that of the normal (uncoded) impulse.

3. The factor K is independent of the modulation signal or the signal frequency deviation.

4. The objective is to minimize the factor K.

The area of the encoded impulse is determined by the step amplitude S_A, step duration $\tau_{\Delta M}$, and impulse duration τ_s. The shape of a typical encoded pulse is shown in figure A-1.

To determine the area under an encoded impulse, it is necessary to determine the amplitude of the encoded impulse in terms of the number of encoding steps or levels N_L. The quantity N_L is an
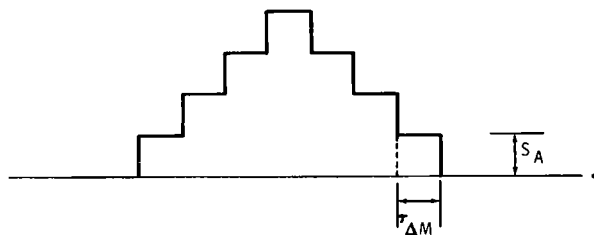

Figure A-1. – Typical encoded pulse shape where $N_L = 4$.

integer and is defined as the ratio of the duration of the noise impulse to the duration of the delta modulator pulse. This is written

$$N_L = \frac{\tau_s}{\tau_{\Delta M}} \tag{A2}$$

defined to the highest integer.

In figure A-1, N_L is equal to 4. The area of the encoded impulse is the sum of the smaller unit areas given by $S_A \tau_{\Delta M}$, which is the area associated with each pulse output from the delta modulator. The total number of unit areas can be considered the sum of an arithmetic progression as given by reference 4.

$$\text{Number of unit areas} = \frac{N_L}{2} (b + c) \tag{A3}$$

where b = number of unit areas $S_A \tau_{\Delta M}$ contained in the first level

c = number of unit areas in the N_Lth level

Therefore, the total area of the encoded pulse is

$$\text{Area}_{\Delta s} = (\text{number of unit areas}) (\text{unit area})$$

$$= \left\{ \frac{N_L}{2} \left[1 + \left(2N_L - 1 \right) \right] \right\} S_A \tau_{\Delta M}$$

$$= N_L^2 S_A \tau_{\Delta M} \tag{A4}$$

Consider now the area of the uncoded impulse. Let the uncoded impulse $I(t)$ be represented by a $\sin x / x$ distribution (ref. 2) such that

$$I(t) = \frac{V_s \sin\left(\frac{2\pi}{\tau_s}\right) t}{\left(\frac{2\pi}{\tau_s}\right) t} \tag{A5}$$

where V_s = amplitude of the output impulse. Integrating $I(t)$, the area is determined to be

$$\text{Area}_s = \frac{V_s \tau_s}{2} \tag{A6}$$

However, the amplitude V_s is not a readily measurable parameter. Considering the $\sin x / x$ distribution, the power associated with the impulse may be written

$$P_{N_s} = \frac{V_s^2 \tau_s}{2} \tag{A7}$$

which, by substituting in equation (A6), is

$$P_{N_s} = \frac{2\left(\text{Area}_s\right)^2}{\tau_s} \tag{A8}$$

The noise power associated with each impulse has been determined previously by equation (7) to be

$$P_{N_s} = (2\pi a)^2 2BW_s \tag{A9}$$

where a is the discriminator constant in V/rad/sec. From equations (A8) and (A9) with $\tau_s \approx 1/BW_s$, the area of an uncoded impulse is

$$\text{Area}_s = 2\pi a \tag{A10}$$

From equations (A2), (A4), and (A10), the noise reduction factor K can be expressed, in terms of measurable parameters, as

$$\sqrt{K} = \frac{\text{Area}_{\Delta s}}{\text{Area}_s} = \frac{\left(\dfrac{\tau_s}{\tau_{\Delta M}}\right)^2 S_A \tau_{\Delta M}}{2\pi a} \tag{A11}$$

47

where $\tau_s/\tau_{\Delta M}$ is defined to the next largest integer. For the SNR tests discussed in the section entitled "Experimental Results," the reduction factor is calculated to be

$$K = \left[\frac{(2)^2(0.039)(2 \times 10^{-6})}{(2\pi)(0.105 \times 10^{-6})} \right]^2 = 0.2 \tag{A12}$$

where $\dfrac{\tau_s}{\tau_{\Delta M}} = \dfrac{4 \times 10^{-6}}{2 \times 10^{-6}} = 2$

$S_A = 0.039 \text{ V}$

$\tau_{\Delta M} = 2 \times 10^{-6} \text{ sec}$

$a = 0.105 \times 10^{-6} \text{ V/rad/sec}$

REFERENCES

1. Rice, S. O.: Noise in FM Receivers. Proceedings, Symposium on Time Series Analysis, M. Rosenblatt, ed., John Wiley & Sons, Inc., 1963, pp. 395-422.

2. Taub, H.; and Schilling, D.: Principles of Communication Systems. McGraw-Hill Book Co., 1971.

3. Dawson, C. T.; Arndt, G. D.; and Batson, B. H.: An Analysis of the Telecommunication Performance of a Data-Relay Satellite System. Vol. 1, Proceedings of the Canaveral Council of Technical Societies, Fifth Space Congress, Cocoa Beach, Fla., Mar. 11-14, 1968, pp. 9.2-1 - 9.2-22.

4. Brink, Raymond W.: College Algebra, Second ed., Appleton-Century-Crofts, Inc. (New York), 1951.

"The aeronautical and space activities of the United States shall be conducted so as to contribute . . . to the expansion of human knowledge of phenomena in the atmosphere and space. The Administration shall provide for the widest practicable and appropriate dissemination of information concerning its activities and the results thereof."

— NATIONAL AERONAUTICS AND SPACE ACT OF 1958

NASA SCIENTIFIC AND TECHNICAL PUBLICATIONS

TECHNICAL REPORTS: Scientific and technical information considered important, complete, and a lasting contribution to existing knowledge.

TECHNICAL NOTES: Information less broad in scope but nevertheless of importance as a contribution to existing knowledge.

TECHNICAL MEMORANDUMS: Information receiving limited distribution because of preliminary data, security classification, or other reasons.

CONTRACTOR REPORTS: Scientific and technical information generated under a NASA contract or grant and considered an important contribution to existing knowledge.

TECHNICAL TRANSLATIONS: Information published in a foreign language considered to merit NASA distribution in English.

SPECIAL PUBLICATIONS: Information derived from or of value to NASA activities. Publications include conference proceedings, monographs, data compilations, handbooks, sourcebooks, and special bibliographies.

TECHNOLOGY UTILIZATION PUBLICATIONS: Information on technology used by NASA that may be of particular interest in commercial and other non-aerospace applications. Publications include Tech Briefs, Technology Utilization Reports and Technology Surveys.

Details on the availability of these publications may be obtained from:

SCIENTIFIC AND TECHNICAL INFORMATION OFFICE

NATIONAL AERONAUTICS AND SPACE ADMINISTRATION
Washington, D.C. 20546